115 (2023) 204993

Contents lists available at ScienceDirect

Gas Science and Engineering

journal homepage: www.journals.elsevier.com/gas-science-and-engineering

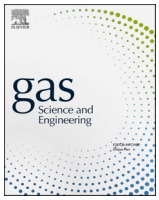

Formation damage and improved recovery in kaolinitic high enthalpy gas fields with fabric geological settings

B. Kanimozhi [a], P. Rajkumar [b], S. Mahalingam [c], S. Senthil [d], D.S. Jayalakshmi [a], H. Girija Bai [a], Vivek Thamizhmani [e], Ramadoss Kesavakumar [f], Venkat Pranesh [f,*]

[a] Fluid Mechanics and Machinery Lab, Sathyabama Institute of Science and Technology, Chennai, Tamil Nadu, India
[b] Advanced Facility for Microscopy and Microanalysis, Centre for Earth Sciences, Indian Institute of Science, Bengaluru, Karnataka, India
[c] Thermal and Heat Transfer Lab, Sona College of Technology, Salem, Tamil Nadu, India
[d] Department of Mechanical Engineering, Kamaraj College of Engineering and Technology, Virudhunagar, Tamil Nadu, India
[e] Department of Petroleum Engineering, Vels Institute of Science, Technology, and Advanced Studies, Chennai, Tamil Nadu, India
[f] Research and Development, DAWN-CALORIFIC, Chennai, Tamil Nadu, India

ARTICLE INFO

Keywords:
Porous media
Rock fabric
Heat transfer fluid
Fines migration
Thermal expansion coefficient
Gas recovery

ABSTRACT

This paper investigates the fines migration and transport in natural gas reservoirs as a function of porous rocks with fabric geological settings. So, an analytical and surface thermodynamic model was developed for high temperature permeable media. Two sets of core flood experiments were conducted under normal (50 °C) and high temperature (150 °C) fluid flow, where the major results revealed that there is an increase in the rock core thermal expansion of 57 ($10^{-6}{}^{\circ}C^{-1}$) and 192 ($10^{-6}{}^{\circ}C^{-1}$) at 50 °C and 150 °C. The rock core underwent a thermal strain to 0.36% and 0.86% under normal and higher temperature conditions. At 50 °C the pressure stabilized to 20 psi and 50 psi was recorded as the peak pressure under 150 °C rock temperature. The fines concentration under higher temperature is significantly higher than the normal rock temperature and yielded maximum up to 77.28 ppm. The rock permeability exhibited a linear and stabilized decline, but at higher temperature new surface energies was created in the rock core and as a result, the reservoir permeability begun to rebound. Microstructural images revealed that the kaolinite clay fine particle under 50 °C has a platelet structure and has multiple straining mechanism. Whereas, under higher temperature the clay fines have transcended to compaction over the rock surface fabrics. Exponential gas recovery of 15% and 25% was observed for both 50 °C and 150 °C cases. In the former case, a linear growth rate to 25% was noted and then gradually it fell to 12.9%. While, in the latter case the gas recovery rate climbed to 33.7% and stabilized, which indicates that the gas recovery rate was monotonous. The experimental and analytical models have been verified using multiple linear regression method and the model's outcome revealed an excellent agreement whose R^2 values were found to be 0.9997 and 0.9995.

1. Introduction

The world is still relying on the fossil fuels for fulfilling their energy needs even after global pandemic Covid-19 (Erias and Iglesias, 2022). Specifically, the natural gas demand is in the exponential growth and this stimulate the natural gas producing companies to explore and produce gas in enormous quantity unlike before from existing and new fields across the globe (Safiyari et al., 2022), and as a result, there is an expansion and optimization of global natural gas supply chain network (Sharma et al., 2021). Moreover, Karakurt and Aydin (2023), analysed the fossil fuels demand and supply in BRICS and MINT nations, and their CO_2 emissions forecasting using Regression Models. Their modelling outcomes indicated that BRICS and MINT countries will dominate the world economy in fossil fuels, especially the natural gas business and they will be the largest emitter of CO_2. Hence, there is a strong outlook for worldwide natural gas demand and it is essential to explore, extract, store, and utilize the existing and new gas reserves for meeting the global energy demand. Enhancing the gas production should be the primary criteria for energy companies and governments. But gas fields containing clay minerals deposits, particularly kaolinite often induce

* Corresponding author.
E-mail address: venkat.pranesh@dawn-calorific.com (V. Pranesh).

https://doi.org/10.1016/j.jgsce.2023.204993
Received 23 October 2022; Received in revised form 15 April 2023; Accepted 20 April 2023
Available online 2 May 2023

reservoir formation damage that is permeability decline and plummet the well production (Prempeh et al., 2020; Kanimozhi et al., 2018; Russell et al., 2017; Zeinijahromi et al., 2012).

Kaolinite clay is ubiquitous and bountiful in oil and gas reservoir rocks (Jiang, 2012). Actually, the layered silicate mineral kaolinite clay ($Al_2Si_2O_5(OH)_4$) is a family of phyllosilicates in which its solid-state chemistry comprises of oxygen atoms bonded with a silica tetrahedral sheet to an alumina octahedral sheet (Kanimozhi et al., 2021) and this clay occurs due to weathering and dissolution of feldspar, which is native to siliciclastic sedimentary rocks (Kanimozhi et al., 2019a). Kaolinite clay is prevalent in sandstone rocks, which is frequently prone to permeability deterioration (Kanimozhi et al., 2020). Although, carbonate rocks are poor in clay minerals, but in some oil and gas carbonate fields kaolinite influencing reservoir triggers permeability decline due to higher grain density, geochemical reactions during permeating fluid flow, temperature, etc (Aoyagi and Chilingarian, 1972). Long back there were field reports of kaolinite presence in carbonate reservoirs, for example Bombay High oil field in India during 1981 (Rao, 1981), and most recently in Malaysian offshore carbonate gas field (Sazali et al., 2020). In general fines are bounded to rock surface and are under the influences of four forces namely, lift (F_l), drag (F_d), electrostatic (F_e) and gravity (F_g). Actually, the F_e *and* F_g hold the clay fine particle over the rock surface, while, F_l *and* F_g detach it from the rock surface (Mahalingam et al., 2019; Zeinijahromi et al., 2016). Generally, fines have a size of order 1 μm (Wang et al., 2012; Raha et al., 2007; Khilar and Fogler, 1998). Commonly, a fine particle over a pore surface is held by a torque balance criterion, as mentioned by the below equation (Yang et al., 2016; You et al., 2016):

$$\frac{\partial(\varphi c+\sigma_s+\sigma_a)}{\partial t}+U\frac{\partial c}{\partial x}=0 \tag{1}$$

where$\sigma_s+\ \sigma_a\ =$ *Concentrations of attached and strained fines*, $U =$ *Darcy velocity*, $c =$ *Volumteric concentration of suspended particles*, $t =$ *time*, $\varphi =$ *Porosity and*, $x =$ *Distance*.

Fig. 1 shows the schematic diagram of fines behaviour in a gas reservoir and Table 1 presents the mathematical conditions for fines attachment and detachment in the permeable media. Due to permeating fluid, temperature, ionic strength, and surface heterogeneity the fines are detached from the rock surface and transport in the porous interspace along with the carrying fluid and in end these fines are captured in the pore-throat and thereby blocking the space for oil, gas, and water transport/recovery to the well, which overall decrease the permeability and surface well production (Zhou et al., 2022; Lin et al., 2021; Trauscht et al., 2015; Schembre and Kovscek, 2005). Furthermore, Russell et al. (2018a,b), conducted laboratory modelling to examine the kaolinite content effects on formation damage in unconsolidated sandstone rocks due to fines migration during low-salinity water injection. The authors have taken five cores for analysis with kaolinite weight percentage ranging from 1% to 10%. The $Al_2Si_2O_5(OH)_4$ along with *NaCl* solutions were sequentially injected in the cores in order to investigate the permeability decline. The major experimental results revealed that kaolinite presence has declined the rock core permeability and also, it was predicted that the rock mineralogy and pore-geometry play a considerable role triggering formation damage. Additionally, Pranesh et al. (2019), investigated the kaolinite fines migration in CBM reservoir at Neyveli Lignite Field, Cauvery Basin, Southern India. The authors conducted a laboratory modelling and analysis for evaluating the formation damage, which includes permeability decline, coal fines production, and structural collapse. Therefore, they conducted three sets of coreflood experiments at ambient conditions. The main results indicated that even at normal room temperature the lignite core has undergone a deterioration in permeability, structural collapse, gas recovery, and increase in coal fines, due to kaolinite clay migration during gas flow.

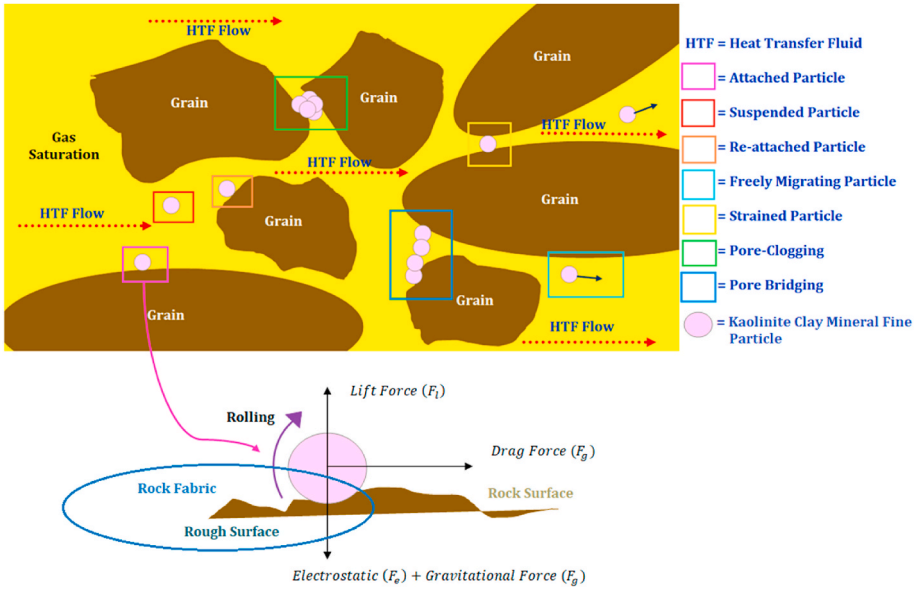

Fig. 1. Schematic diagram of fines migration in permeable rock media with fabric rock formation during gas flow. For enlarged view of image, the reader is advised to see the appendix.

Table 1
Mathematical condition for fines attachment and detachment from the rock surface.

Case No.	Fines Concentration	Fines State	Fines Force
Case 1	$(F_l+F_d)>(F_g+F_e)$	Oversaturated Fines	Start of Detachment and Migration
Case 2	$(F_l+F_d)<(F_g+F_e)$	Undersaturated Fines	Surface Attachment Period

$F_l =$ *Lift Force*, $F_d =$ *Drag Force*, $F_g =$ *Gravitational Force*, *and* $F_e =$ *Electrostatic Force*

Specifically, the kaolinite clay mineral fine particle structure, in this case it is flake (geometry) has strained the rock cleats and pore-throat, and causing permeability decrease. Hence, it is emphasized that all gas fields are prone to reservoir formation damage under the existence of kaolinite clay.

On other side, there were early reporting of positive aspects of fines migration (mostly clay minerals-kaolinite in specific) in which fines assist in the recovery of oil, gas, and water by fluid flow diversion, subsurface strata structure and wettability alterations (Borazjani et al., 2017; Hussain et al., 2013; Zeinijahromi et al., 2011). For instance, Nguyen et al. (2013), studied the fines-migration-assisted improved gas recovery during gas field depletion. Authors have applied the concept of permeability deterioration in order to reduce the production of water during gas field depletion. Their concept and aim are to decelerate the intruding the aquifer water by injection of a little volume of fresh water into an abandoned watered-up well. They have derived an equation for the immiscible compressible two-phase fluid with fines mobilization and capture. Those equations are transformed to the black-oil polymer flooding model in large scale approximation. The fresh water bank injection considerably improves the gas recovery and reduces the production of water, which was revealed in reservoir simulation modelling results. Moreover, in a recent study, Mehdizad et al. (2022) performed a visual inspection and analysis on the effects of clay-induced fluid flow diversion on oil recovery, as a mechanism of low salinity water flooding. The authors conducted an investigation on sandstone rocks in order to increase the oil recovery with help of fines migration. The results shows that the during low salinity water flooding the clay fines has undergone swelling and migration. There was a wettability alteration and fluid diversion phenomenon, which lead to incremental oil recovery. Ultimately, the authors claim that presence of clay in reservoirs is essential in order to enhance the oil production.

Gas bearing reservoir rocks are of high enthalpy, which means having huge amount of heat contents in other words it is called a thermal potential (Pranesh and Ravikumar 2019). Mostly, rock enthalpy is often spoken and associated with geothermal rocks (High and Low Enthalpy), but it is also applicable to oil and gas reservoirs. During water and CO_2 injection in oil and gas reservoirs the fluids act as a heat transfer fluid, which liberates the heat (enthalpy) from the rock to assist in the sweep, transport, and recovery. But this scenario frequently causes formation damage. However, in this paper the reservoir gas act as a heat transfer fluid (HTF) and actually HTF is a gas or liquid that participate in the process of transferring heat to the designed medium or phase reaction. Its main role is to transport and store the thermal energy (Kanimozhi et al., 2017, 2019b; Weiguo et al., 2016; van der Stelt et al., 2015). Actually, HTF is a fascinating concept, which is common and popular energy acceleration method in mechanical and thermal engineering fields, but to our best of our knowledge this technique is not applied and almost unprecedented to the reservoir engineering community. So, this paper makes an audacious attempt to analyse the fines behaviour and improved gas recovery in porous sandstone rock with fabric geology.

Rock fabric or fabric theory is fundamentally indicating the rock pattern and actually, it is an arrangement of elements such as textures, layers, fossils, and minerals that make up the rock (Gokhale, 2019; Singh, 2013; Wall, 2006; Ghosh, 1993). Geologic fabric theory describes the spatial and geometric configuration of rock texture which includes surface roughness, cleats, cracks, fissure, and fractures (Hobbs et al., 1976). In reality, all reservoir porous rocks are fabric in nature and to be specific, its pore walls have fabric design (Britannica, 2022; Hills, 1963; Davis et al., 2011; Fossen, 2010). Its major types are primary, shape, crystallographic, S-fabric, L-fabric, and penetrative fabric (Twiss and Moores, 2007). However, in this paper the rock fabric denotes the surface roughness or technically speaking the rock fabric is a function of surface roughness. Fig. 2 presents the general rock expansion coefficient with respect to increasing temperature at normal and high temperature during gas and heat flow. This research just focuses on the shape fabric and penetrative fabric. Actually, the former deals with the specific rock's inequant elements orientation and structures, and the latter describes about the grain scale that is the entire rock is composed of fabric (Passchier and Trouw, 2005).

In certain research, surface roughness parameter is seen as a

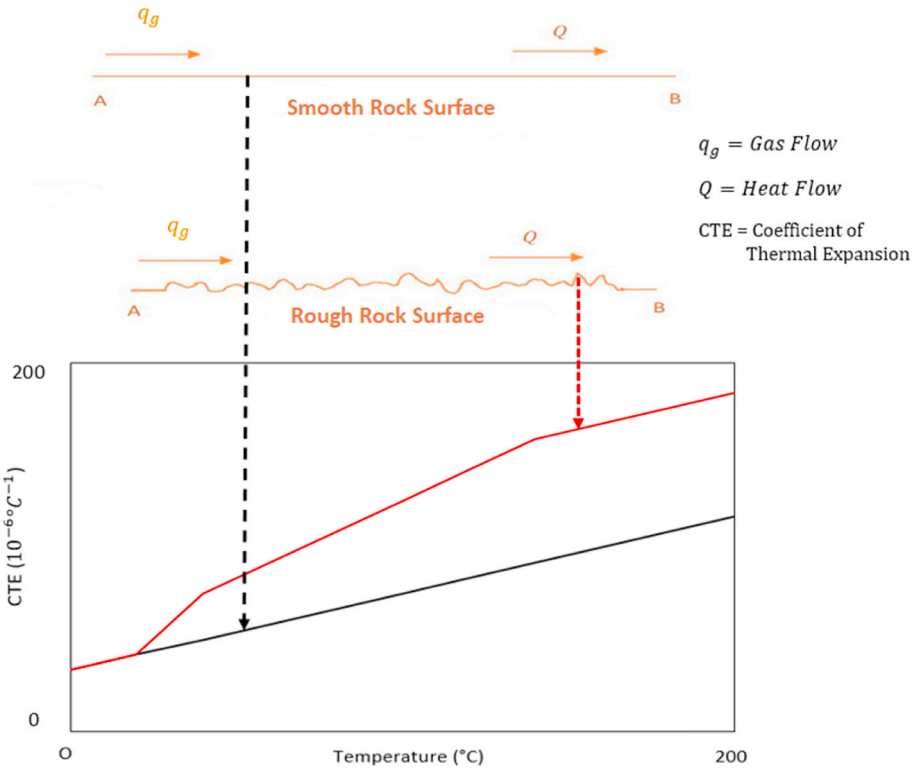

Fig. 2. Rock expansion coefficient with respect to increasing temperature. For enlarged view of image, the reader is advised to see the appendix.

potential influencer in fluid flow pattern, particle retention, wettability alteration, and fracture creation (Zhang et al., 2021; You and Lee, 2021; Li et al., 2021; Geistlinger et al., 2016; Argent et al., 2015). Literally, Huang et al. (2022) analysed the surface roughness influences on methane flow in shale kerogen nano-slits. Actually, the authors conducted numerical simulations to evaluate the velocity and mass flow rate of CH_4 flow in nano-pores of real kerogen. Also, a new mathematical model was developed to quantify this phenomenon and their results showed that the transport phenomena is largely affected and the authors emphasize that it is critical and vital to understand the methane flow mechanism in kerogen nano pores for accurate evaluations of gas recovery in shale formations. Obviously in cases like this there would be a heat dissipation and thermal diffusivity. For instance, Askari et al. (2018) studied the thermal conductivity in deforming isotropic and anisotropic granular porous media with rough grain surface. The authors examines that the porous materials (grain) with rough surface would undergo a deformation to a compressing pressure. Single fluid saturated porous media affects the grain conductivity, size (geometry) and shall deform. Moreover, the thermal conduction is largely influenced by surface roughness and porosity. Also, larger anisotropy appears when the granular porous media is at the function of surface roughness.

Therefore, the main objective of this paper is to evaluate and quantify the sequential formation damage and subsequent, gas recovery in sandstone rock with rough pore surface during single-phase fluid flow. Furthermore, to investigate the kaolinite fine particle geometry and propose a formation damage mechanism, and also, to support and claim the necessity of kaolinite presence in gas reservoirs for enhanced gas recovery.

2. Surface thermodynamic modelling of porous rocks: analytical model

2.1. Thermodynamics of wettability

Naik et al. (2015), studied the influence of wettability alteration on rate enhancement in unconventional gas reservoirs. Firstly, the authors analysed the water blockage problem due to the capillary end effect near the fracture face and vicinity of wellbore is a potential threat to gas production. They have proposed a solution to this problem by alteration in wettability which can also be applied to dewater acceleration and prevention in the drilling fluid leak off. Since rock surface wettability change to less water wet results in capillary pressure reduction and water blockage reduction effects. Authors have developed an analytical model for steady state two-phase linear and radial flows and accounting for contact angle dependent relative permeability and capillary pressure. Their model was validated with laboratory data and showed good agreement. Ultimately, their modelling showed that the maximum well productivity indexes for water and gas in an optimal contact angle is in the competition between capillary and viscous effects. Even, the authors have proposed the injection of nanoparticle for wettability modification in unconventional rocks and typically, after dewatering it makes the rock more water-wet that leads to displacement of water into tiny pores with subsequent increase in gas rate. But, this model on wettability alteration to enhance the gas production in low permeable rocks lacks thermodynamic explanation and relationship establishment on fines and fluid wettability alteration and migration. Heat accumulation and transfer, and enthalpy of unconventional rocks may influence the water blockage phenomenon. Besides, Schembre et al., 2006, investigated the impact of water imbibition on wettability alteration and oil recovery at high reservoir temperature. Primarily, their investigation assumes the wettability is the function of temperature and have used the DLVO theory to calculate colloidal stability and to interpret the lab-scale displacement results. Generally, forces acting between fines and rock surface is either attractive or repulsive and this determines the colloidal stability balance. When compared to electrolyte ions colloidal particles are assumed to be large and this allows to establish a forces of interaction between a fine and surface denoted as F_T as a function of mutual separation.

$$F_T(h) = F_A(h) + F_R(h) \tag{2}$$

where, h is the ratio of distance of separation and F_A and F_R are attractive and repulsive forces as per DLVO theory. Calculations for attraction of particle onto a rock surface, the London van der Waals can be applied using the below equation (Hamaker, 1937):

$$V_{LVA}(h) = -\frac{A}{6}\left[\frac{2(h+1)}{H(H+2)} + \ln\left(\frac{H}{H+2}\right)\right] \tag{3}$$

in the above equation A indicates the Hamaker constant. While, calculation for particle repulsion from pore surface in an assumption of constant surface charge can be complied with an assistance from electric double layer repulsion, which is mathematically mentioned below:

$$V_{DLR}(h) = \frac{\varepsilon r_p}{4}\left(\varphi_{01}^2 + \varphi_{02}^2\right)\left[\left(\frac{2\varphi_{01}\varphi_{02}}{\varphi_{01}^2 + \varphi_{02}^2}\right)\right] \times \ln\left(\frac{1+\exp(-kh)}{1-\exp(-kh)}\right) - \ln(1 - exp(-2kh)) \tag{4}$$

Where ε is the dielectric constant of porous medium and φ_{01} and φ_{02} are the pore wall and particle surface potentials and r_p is the particle radius, and k is length given by the Debye-Huckel reciprocal:

$$k = \sqrt{\frac{2e^2 n_b}{\varepsilon\, k\, T}} \tag{5}$$

n_b is the bulk total ion density and authors assumed and associated all variables with the function of temperature. In temperature viewpoint, it is assumed to be repulsive and authors have successfully demonstrated this effect by considering fluid and particle wettability as a dominant factor. They performed water imbibition tests with nine diatomaceous reservoir rock cores and k and φ varied from 0.2 to 0.7 md and 46–65% respectively. Experiments conducted spontaneous counter current water imbibition and then followed by forced cocurrent water imbibition to residual oil saturation. The fluids were synthetic formation brine and crude oil with 34°API. The temperature ranged from 45 to 230 °C at sufficient pressure to maintain the water. The outcome of experimentations indicated that wettability alteration as a function of elevated temperature is the key factor in fines detachment and reveals substantial growth in imbibition rate and oil recovery. Also, it was observed a slight decrease in water wet and fines release coated with crude oil exposes clean water wet pore surfaces. On the whole, DLVO calculations elucidate fine particle detachment from the surface of the pore at elevated in-situ reservoir temperature.

2.2. Slow mobilization of fines over rock surface

Yang et al. (2016), analysed the detached fines slow migration over the rock surface in porous media. Many coreflood experiments have indicated that the permeability stabilization time accounts for hundreds of PVI and the theory of classical filtration accepts that the released fines particles are migrated by carrier fluid in bulk form and causing permeability stabilization after one PVI. Authors have given much importance to stabilization periods for reducing the fines mobilization drift near pore walls. They developed an analytical model for one dimensional flow along with fines discharge and straining under piecewise-constant velocity. Also, they proposed basic equation for flow of single phase particle movement in porous rock with velocity lower the velocity of carrier fluid. Even though, their modelling is in good agreement with laboratory data, it lacks analytical investigation with regards to wettability and surface thermodynamics. Actually, the intermolecular forces acting between two particles can be written as follows (Raman et al., 2016):

$$F_i = \frac{\partial}{\partial_j}\left(\rho C_s^2 - P\right)\partial_{ij} + k\rho\frac{\partial}{\partial x_i}\frac{\partial^2}{\partial x_j}\frac{\rho}{\partial x_j} \tag{6}$$

where k is a constant and is related to surface tension magnitude and Fi the intermolecular force comprises of phase separating force that relies on non-ideal equation of state and force of surface tension. The modelling can be extended with respect to surface heat and thermodynamic pressure distributions. Also, Oliveira et al. (2014), studied this same phenomenon of slow mobilization of reservoir fines in porous media and specifically, authors have reported from experiments that the speed of mobilized fines drift is considerably lower than the carrier fluid (water) velocity. It should be noticed that this fine drifting can be a sum of different particle micro motions like rolling over the surface of rock and sliding in the walls of the rock pores.

2.3. Wettability influence on fines migration in porous media

Wettability is an ability of fluid or particle to maintain contact with the rock surface and is generally measured by contact angle between the tangent drawn at the triple point between the three phases such as solid, liquid, gas and the substrate surface. Surface roughness has a potential impact on the alternation of particle wettability (Kumar and Prabhu, 2007). The wetting behaviour of liquid on solid is sensitive to temperature variation as temperature influences the liquid properties and substrate and it is a statement that soaring temperature reduces the liquid viscosity and surface tension and also in reactive wetting systems the diffusion rate generally rises with temperature increase (Bernardin et al., 1997). The wettability is an interaction between rock-vapor surface tension, γ_{sv} and rock-liquid surface interfacial tension, γ_{sl}. The general measure of contact angle for liquid and solid particle is given by the Young's equation (Alshakhs and Kovscek 2016):

$$\gamma_{lv}\cos\theta = \gamma_{sv} - \gamma_{sl} \tag{7}$$

and an EOS for interfacial tensions can be written as (Yuan and Randall Lee, 2013):

$$\gamma_{sl} = f(\gamma_{lv}, \gamma_{sv}) \tag{8}$$

Additionally, Gibb's Thermodynamics of Wetting states that the interface between solid and fluid phase can be split into two parts, one fitting to solid and the other belonging to the fluid. Consistently, the interface forming work can be mentioned as the total work (ω) of forming solid surface in a vacuum and the forming work (ρ) of the fluid part of the interface. The quantity (ρ) called by Gibbs superficial tension of a fluid in contact with the solid. This can be treated as energy or as a force like the liquid surface tension (Toshev, 2006). The Gibbs solid-liquid adsorption equation is given by

$$d\omega = -S_s dT + (\sigma - \omega)\, dA/_A - \sum_i \Gamma_i d\mu_i \tag{9}$$

However, the above solid adsorption equation didn't account for solid surface roughness. But, this paper takes the role of surface roughness influence on natural fine particle wettability and migration into a consideration. To illustrate the geologic fabric theory with respect to fluid and particle flow in a simple way, consider Fig. 2. One dimensional smooth surface with ends A and B and there is a flow of water and heat at high velocity. We have even assumed that smooth surface has varying thermal conductivity and in that there is no change in the reduction of liquid flow velocity. This is because the smooth surface having no resistance to flow. For smooth surface there is a rate of change of surface free energy that is given by Frenkel's approach:

$$\frac{dF}{dt} = 2\pi\gamma_{1v}[\cos\theta - I]r_o v_E \tag{10}$$

For rough surface is given by

$$\frac{dF}{dt} = 2\pi\gamma_{1v}[\cos\theta - rI]r_o v_E \tag{11}$$

in rough rock surface, with assumption of same parameters, there will be a reduction in fluid velocity due to high intensity surface roughness (linear and continuous variation in the surface). Because of rugged surface, there will be a high thermal conductivity and this may govern the slow mobilization of fluid. Now consider fine particles, which is transported in the suspension form and with impacts of surface roughness, the fines particles will be drifting and colliding in the surface materials. It takes more time to reach the point B. Therefore, the rock fabrics or surface roughness together with thermal conductivity determines the particle wettability and slow mobilization in porous media (Wu et al., 2016; Gu et al., 2016). Khanna (2014) stated that there are many ways of expressing surface roughness numerically, but the following two methods are commonly used:

1) Centre line average (CLA) method, and
2) Root mean square (RMS) method

CLA is defined as the average value of the ordinates (distance between two rock teeth) between the surface and mean line, measure on both sides of it. Mathematically it is defined as below:

$$CLA = \frac{y_1 + y_2 + y_3 \ldots\ldots y_n}{n} \tag{12}$$

where, y_1, y_2, ……y_n are the ordinates measured on both sides of the mean line and n are the number of ordinates.

The RLA is defined as the square root of the arithmetic mean of the squares of the ordinates, mathematically expressed as:

$$RMS = \sqrt{\frac{y_1 + y_2 + y_3 \ldots\ldots y_n}{n}} \tag{13}$$

2.4. Impact of particle wettability on slow mobilization of fines in porous rocks

For modelling purpose, we assume that the grain surface structure is convex. So a fine particle resting on the convex grain surface have the following expression from capillary fall:

$$h = \frac{4\sigma\cos\theta}{\rho g d} \tag{14}$$

$$h\rho g d = 4\sigma\cos\theta$$

$$\cos\theta = h\rho g d$$

$$\theta = \cos^{-1}(h\rho g d) \tag{15}$$

equation (15) is the contact angle for fine particle wettability. Where h is height of the fine particle height that is from top axis to bottom of the rock surface, ρ and g are the density and gravitational force (value 9.8) of the particle, and d is the diameter. Since we assume fine particle is in a sphere shape, so these parameters will be applicable.

If the surface roughness is taken into consideration, then by equating, we get

$$\theta = CLA$$

$$\cos^{-1}(h\rho g d) = \frac{y_1 + y_2 + y_3 \ldots\ldots y_n}{n}$$

$$\theta = \cosh\rho g d\left[\frac{y_1 + y_2 + y_3 \ldots\ldots y_n}{n}\right] \tag{16}$$

For RMS,

$$\theta = cosh\ \rho g d \sqrt{\frac{y_1 + y_2 + y_3 \ldots\ldots y_n}{n}} \tag{17}$$

Therefore, equation (16) or 17 can be used to find the fine particle wettability contact angle with respect to surface roughness.

2.5. Heat of fine particle immersion in porous media

Immersion of fine particles in fluid influx is generally accompanied by the release of heat known as heat of immersion (ΔH_i). This is defined as the heat liberated from material surface per square centimeter of the particles immersed in the liquid/gas, and is related to the contact angle of the particles (Kanimozhi et al., 2019b; Senthil et al., 2019; Neumann et al., 2011). Hence, it is also possible to characterize the fine particle wettability through measurement of heat of immersion. But, in this modelling, we are considering the influence of surface roughness (R_∇). Therefore, we must include this factor in this derivation.

The free energy of immersion (ΔF_i) of the fine particles can be mentioned as:

$$\Delta F_i = R_\nabla(\gamma_{sl} - \gamma_{sv}) \tag{18}$$

Where γ_{sl} and γ_{sv} are the rock-liquid and rock-vapor/gas surface tensions of the fine particles respectively. equation (18) indicates that these factors are functions of the rock surface roughness.

Combining young's equation with Equation (18) gives

$$\Delta F_i = -R_\nabla(\gamma_{lv}\ cos\ \theta) \tag{19}$$

The enthalpy of immersion (ΔH_i), that is, the heat of immersion at variable temperature and volume is related to ΔF_i, given by

$$\Delta H_i = \Delta F_i + R_\nabla + \Delta S\ dT = \Delta F_i - R_\nabla \frac{d\Delta F_i}{dT} \tag{20}$$

where, S is the entropy, and dT is the change in pore temperature. Substituting equation (19) in equation (20) gives:

$$\Delta H_i = R_\nabla \frac{dR_\nabla(\gamma_{lv}\ cos\ \theta)}{dT} - R_\nabla(\gamma_{lv}\ cos\ \theta)$$

$$\Delta H_i = R_\nabla \left[\frac{dR_\nabla(\gamma_{lv}\ cos\ \theta)}{dT} - (\gamma_{lv}\ cos\ \theta)\right] \tag{21}$$

Equation (21) can be written as:

$$\cos\theta = \frac{R_\nabla\left[\frac{dR_\nabla(\gamma_{lv}\ cos\ \theta)}{dT} - \Delta H_i\right]}{\gamma_{lv}} \tag{22}$$

Equation (22) can be solved numerically to determine the contact angle from the heat of immersion. ΔH_i can be measured using calorimeter. Though, the heat of immersion method consists many serious complications: firstly, the specific surface area of the particles with respect to roughness should be known. Surface roughness of rock surface can be measured by Taylor Hobson Surface Roughness Tester. Secondly, an engineer needs to ensure that experimental heat of immersion is indeed the heat of wetting, and that there are no contributions from the partial dissolution of particles. Third, the heat of wetting that is an enthalpy is not only related to contact angle (a quantity of free energy), but also to the temperature dependence of the contact angle. It is extremely difficult to gather details on temperature dependence of the contact angles without already knowing the contact angle value. According to modified Young's equation, $dR_\nabla(\gamma_{lv}\ cos\ \theta)/dT$ in equation (22) can be approximated by the temperature dependence of the rock surface tension with regards to roughness; that is, $R_\nabla\left(\frac{d\gamma_{sv}}{dt}\right)$. The value of this expression can vary from different rock surface fabrics, depending upon the field and geology. Therefore, the heat of immersion technique will usually only give semiquantitative and relative details.

2.6. Slow mobilization of fines with regards to rock surface roughness

Let us derive an analytical expression for suspension flow velocity with respect to surface roughness. Let us take capillary bundle porous geometry with mixing chambers for modelling. Considering following parameters for modelling:

Let,

H_1 = Height of the fluid on the point of top ordinate in the pore mixing chamber.

H_2 = Height of the fluid on the bottom point of ordinate in the pore mixing chamber.

H = Difference in the fluid level

B = Width of ordinate.

R_∇ = *Surface roughness either CLA or RMS Equation.*

Fluid height above the ordinate of the pore mixing chamber.

$$= H_1 + \frac{H_2 - H_1}{2} = \frac{H_1 + H_2}{2} \tag{23}$$

Fluid flow level at the bottom of the pore mixing chamber ordinate

$$= \frac{H_1 + H_2}{2} - H \tag{24}$$

By applying Bernoulli's equations (23) and (24), we get

$$\frac{p_1}{\rho g} + \frac{V_1^2}{2g} = \frac{p_2}{\rho g} + \frac{V_2^2}{2g} \tag{25}$$

Now,

$$\frac{p_1}{\rho g} = \frac{H_1 + H_2}{2}, \frac{p_2}{\rho g} = \frac{H_1 + H_2}{2} - H + \frac{V_2^2}{2g}$$

And V_1 is negligible, then

$$\frac{H_1 + H_2}{2} + 0 = \frac{H_1 + H_2}{2} - H + \frac{V_2^2}{2g}$$

Therefore,

$$\frac{V_2^2}{2g} = H$$

$$V_2 = \sqrt{2gH} \tag{26}$$

Width of the ordinate $= b(H_2 - H_1)$.

Thus, the change in fluid flow from pore mixing chamber to pore throat would be

$$\Delta q_w = R_\nabla \times b(H_2 - H_1) \times \sqrt{2gH} \tag{27}$$

The above equation can be used for change in the fluid flow in porous media with regards to surface roughness. Now we will include the heat flow factor in this problem and the fine particle will only vary if there is a variation in thermal conductivity of rock surface. So, at uniform heat conduction, the particle will only oscillate on the rugged surface.

Now, assume that heat flow rate is given by

$$Q = \frac{K\Delta T}{\sqrt{\pi\alpha}} \tag{28}$$

Heat received by the rock surface at temperature T_1 is

$$Q_1 = \frac{K(T_1 - T_s)}{\sqrt{\pi\alpha_1}} \tag{29}$$

Heat lost by the surface of rock at temperature T_2 is

$$Q_2 = \frac{K(T_s - T)}{\sqrt{\pi\alpha_2}} \tag{30}$$

We know that $\alpha = \frac{k}{c}$.

The fine particle will remain in the contact rough surface only at

constant temperature and it is demonstrated below:

$$\frac{k(T_1 - T_s)}{\sqrt{\pi\alpha_1}} = \frac{k(T_s - T_2)}{\sqrt{\pi\alpha_2}}$$

Or,

$$\frac{k(T_1 - T_s)}{\sqrt{\alpha_1}} = \frac{k(T_s - T_2)}{\sqrt{\alpha_2}}$$

$$k_1(T_1 - T_s)\sqrt{\alpha_2} = k(T_s - T_1)\sqrt{\alpha_1}$$

$$k_1 T_1\sqrt{\alpha_2} - k_1 T_s\sqrt{\alpha_2} = k_2 T_s\sqrt{\alpha_1} - k_2 T_2\sqrt{\alpha_1}$$

$$T_s(k_1\sqrt{\alpha_2} + k_2\sqrt{\alpha_1}) = k_1 T_1\sqrt{\alpha_2} + k_2 T_2\sqrt{\alpha_1}$$

$$T_s = \frac{\left(k_1 T_1/\sqrt{\alpha_1}\right) + \left(k_2 T_2/\sqrt{\alpha_2}\right)}{\left(k_1/\sqrt{\alpha_1}\right) + \left(k_2/\sqrt{\alpha_2}\right)} \tag{31}$$

Therefore, the above equation accounts for fine particle mechanical stability under isothermal regime. The fines balance equation and sink source of the attached/detached and strained fines is given by (Coronado and Diaz-Viera, 2017):

$$\varphi\frac{\partial C_m}{\partial t} + (1-\varphi)\frac{\partial\left(\chi_f\sigma_a + \sigma_c\right)}{\partial t} + \nabla.\left[UC_m - D_{Lf}\nabla C_m\right] \tag{32}$$

Where σ_a is the attached fines concentration (mass/volume), σ_c is the clogging fines concentration that mass per unit volume. $D_{Lf} = \alpha_{Lf}U$ is the longitudinal dispersion coefficient of the mobile fines, α_{Lf} is the longitudinal fines dispersivity, and χ_f is the mass fraction of the rock which release fine particles. Now let us handle the problem of porous surface roughness thermal conductivity. Now we derive an expression for total heat flow through rough porous surface. The varying temperature in porous media is given by:

$$K = K_0\left(1 + \alpha t + \beta t^2\right) \tag{33}$$

Considering a steady state conduction in capillary bundle porous rocks with the radius r = r and the temperature varies with increasing roughness $\left(\frac{dR_\nabla}{dt}\right)$, we can write the equation as below:

$$Q = -KR_\nabla\frac{dt}{dr} \tag{34}$$

Substituting the given value of K in equation (34), we get

$$Q = -K_0\left(1 + \alpha t + \beta t^2\right)R_\nabla\frac{dt}{dr} \tag{35}$$

$$\frac{Q}{R_\nabla} \times \mathrm{dr} = = -K_0\left(1 + \alpha t + \beta t^2\right)dt$$

Integrating the above equation in the given range, we get

$$\frac{Q}{R_\nabla}\int_{r_1}^{r_2} dr = -K_0\int_{t_1}^{t_2}\left(1 + \alpha t + \beta t^2\right)dt$$

in the above equation it is mentioned as integral from r_1 to r_2 and t_1 to t_2, it indicates that radius of pore mixing chamber to capillary tube, and initial temperature to final temperature.

$$\frac{Q}{R_\nabla}[dr]_{r_1}^{r_2} = -K_0\left[\left(t + \alpha\frac{t^2}{2} + \beta\frac{t^3}{3}\right)\right]_{t_1}^{t_2}$$

$$\frac{Q}{R_\nabla}\left(\frac{1}{r_2} - \frac{1}{r_1}\right) = K_0\left[(t_2 - t_1) + \alpha\left(\frac{{t_2}^2 - {t_1}^2}{2}\right) + \frac{\beta}{3}\left({t_2}^3 - {t_1}^3\right)\right]$$

$$\frac{Q}{R_\nabla}\left(\frac{r_1 - r_2}{r_1 r_2}\right) = -K_0\left[(t_1 - t_2) + \frac{\alpha}{2}\left({t_1}^2 - {t_2}^2\right) + \frac{\beta}{3}\left({t_1}^3 - {t_2}^3\right)\right]$$

$$\frac{Q}{R_\nabla}\left(\frac{r_2 - r_1}{r_1 r_2}\right) = -K_0(t_1 - t_2)\left[1 + \frac{\alpha}{2}(t_1 + t_2) + \frac{\beta}{3}\left({t_1}^2 + t_1 t_2 + {t_2}^2\right)\right]$$

$$Q = \frac{R_\nabla r_1 r_2}{r_2 - r_1} \times K_0(t_1 - t_2)\left[1 + \frac{\alpha}{2}(t_1 + t_2) + \frac{\beta}{3}\left({t_1}^2 + t_1 t_2 + {t_2}^2\right)\right] \tag{36}$$

Thus, the above expression can be applied for the heat flow over rough porous surface. If the thermal conductivity of the porous rough surface varies according to the following relation:

$$K = K_1 + (K_2 - K_1)[(t - t_1)/(t_2 - t_1)] \tag{37}$$

Now, by substituting the above value in equation (35), we get:

$$Q = -[K_1 + (K_2 - K_1)\{(t - t_1)/(t_2 - t_1)\}]R_\nabla\frac{dt}{dr}$$

$$Q.\frac{dr}{r^2} = -R_\nabla[K_1 + (K_2 - K_1)\{(t - t_1)/(t_2 - t_1)\}]\frac{dt}{dr} \tag{38}$$

Integrating both sides, we get

$$Q\int_{r_1}^{r_2}\frac{dr}{r^2} = -R_\nabla\int_{t_1}^{t_2}\left[K_1 + (K_2 - K_1)\left\{\frac{t - t_1}{t_2 - t_1}\right\}\right]dt$$

$$-Q\left[\frac{1}{r}\right]_{r_1}^{r_2} = -R_\nabla\left[K_1 t + \frac{K_2 - K_1}{t_2 - t_1}\left\{\frac{t^2}{2} - t.t_1\right\}\right]_{t_1}^{t_2}$$

$$-Q\left[\frac{1}{r_2} - \frac{1}{r_1}\right] = -R_\nabla\left[K_1(t_2 - t_1) + \frac{K_2 - K_1}{t_2 - t_1}\left(\frac{{t_2}^2 - {t_1}^2}{2}\right) - t_1\left(\frac{K_2 - K_1}{t_2 - t_1}\right)(t_2 - t_1)\right]$$

$$Q.\frac{(r_2 - r_1)}{r_1 r_2} = -R_\nabla\left[K_1(t_2 - t_1) + \frac{K_2 - K_1}{2}(t_2 - t_1) - t_1(K_2 - K_1)\right]$$

$$= -R_\nabla\left[K_1(t_2 - t_1) + \frac{K_2 - K_1}{2}(t_2 + t_1 - 2t_1)\right]$$

$$= -R_\nabla\left[K_1(t_2 - t_1) + \frac{K_2 - K_1}{2}(t_2 - t_1)\right]$$

$$= -R_\nabla(t_2 - t_1)\left[K_1 + \frac{K_2 - K_1}{2}\right]$$

$$Q = R_\nabla(t_2 - t_1)\left(\frac{K_1 + K_2}{2}\right)\left(\frac{t_1 - t_2}{r_2 - r_1}\right) \tag{39}$$

This is the derived and required expression for varying thermal conductivity in porous surface with irregular surface roughness.

2.7. Well production decline due to fines straining migration fabric theory perspective

For modelling the well productivity decline due to fines migration in fabric theory viewpoint, first we need to model the temperature distribution in the porous media having roughness characteristics. Generally, fines get displaced by carrier fluid and in that some of fine particles are being suspended. From the angle of thermodynamics, the variation in porous medium heat transfer and porous surface thermal conductivity detaches the fine particles from the rock surface. Due to the existence of surface roughness it takes long time for suspension to get strained in pore throat. Even in the slow mobilization of fines process, well productivity decline will occur. In this modelling also, we will take the capillary bundle porous medium with mixing chambers standard model. Now, we will consider the radial conduction and axial enthalpy transport in the porous media, we have:

Thermal conduction into the porous mixing chamber

$$Q_r = -k(R_\nabla.dx)\frac{\partial t}{\partial r} \tag{40}$$

Heat conducted out of the porous mixing chamber

$$dQ_{r+dr} = -K\left[R_\nabla\,(r+dr)dx\frac{\partial}{\partial x}\left(t+\frac{\partial t}{\partial r}dr\right)\right] \tag{41}$$

Net heat convected out of the pore mixing chamber,

$$dQ_{conv} = \rho R_\nabla u c_p \frac{\partial t}{\partial r}dx \tag{42}$$

Considering energy balance on the porous chamber, we obtain

$$(Heat\ conducted\ in)_{net} = (Heat\ conducted\ out)_{net}$$

$$dQ_r - dQ_{r+dr} = (dQ_{conv})_{net} \tag{43}$$

$$-KR_\nabla\frac{\partial t}{\partial r} - \left[-K\left\{R_\nabla(r+dr)dx\frac{\partial}{\partial r}.\left(t+\frac{\partial t}{\partial r}dr\right)\right\}\right] = \rho R_\nabla druc_p\frac{\partial t}{\partial x}dx$$

$$-KR_\nabla\frac{\partial t}{\partial r} + K\{R_\nabla(r+dr)\}dx\left[\frac{\partial t}{\partial r}+\frac{\partial^2 t}{\partial r^2}dr\right] = \rho R_\nabla druc_p\frac{\partial t}{\partial x}dx$$

$$-KR_\nabla\frac{\partial t}{\partial r} + K\left(R_\nabla dx.\frac{\partial t}{\partial r}\right) + K\left(R_\nabla dx.\frac{\partial^2 t}{\partial r^2}dr\right) + K(R_\nabla drdx)\frac{\partial t}{\partial r} + K\left(R_\nabla drdx.\frac{\partial^2 t}{\partial r^2}dr\right) = \rho(R_\nabla.dr)uc_p\frac{\partial t}{\partial x}dx$$

Neglecting second order terms, we get

$$K\left(\frac{\partial t}{\partial r}+r\frac{\partial^2 t}{\partial r^2}\right)dx.dr = \rho R_\nabla uc_p\frac{\partial t}{\partial r}dr \tag{44}$$

$$\frac{1}{r}\frac{\partial}{\partial r}\left(r\frac{\partial t}{\partial r}\right) = u\frac{\rho c_p}{K}\frac{\partial t}{\partial x}$$

$$\frac{1}{r}\frac{\partial}{\partial r}\left(r\frac{\partial t}{\partial r}\right) = \frac{u}{\alpha}\frac{\partial t}{\partial x} \tag{45}$$

By inserting the value of maximum velocity distribution $u = u_{max}\left[1-\left(\frac{r}{R}\right)^2\right]$ in the above equation, we get:

$$\frac{1}{r}\frac{\partial}{\partial r}\left(r\frac{\partial t}{\partial r}\right) = \frac{1}{\alpha}\frac{\partial t}{\partial x}.u_{max}\left(1-\frac{r^2}{R^2}\right) \tag{46}$$

$$\frac{\partial}{\partial r}\left(r\frac{\partial t}{\partial r}\right) = \frac{u_{max}}{\alpha}.\frac{\partial t}{\partial x}.\left(r-\frac{r^3}{R^2}\right)$$

Let us consider heat flux along the porous rough surface, then

$$r\frac{\partial t}{\partial r} = \frac{1}{\alpha}\frac{\partial t}{\partial x}u_{max}\left(\frac{r^2}{2}-\frac{r^4}{4R^2}\right) + R_\nabla \tag{47}$$

$$\frac{\partial t}{\partial r} = \frac{1}{\alpha}\frac{\partial t}{\partial x}u_{max}\left(\frac{r^2}{2}-\frac{r^4}{4R^2}\right) + \frac{R_\nabla}{r}$$

Integrating again, we have the following expression

$$t = \frac{1}{\alpha}\frac{\partial t}{\partial x}u_{max}\left(\frac{r^2}{2}-\frac{r^4}{4R^2}\right) + C_1R_\nabla\ln(r) + C_2 \tag{48}$$

Where C_1 *and* C_2 are the constants of integration

The boundary conditions are:

At r = 0, $\frac{\partial t}{\partial r} = 0$

At r = R t = t_s

Applying the above boundary conditions, we get

$$C_1 = 0, C_2 = t_s - \frac{1}{\alpha}\frac{\partial t}{\partial x}u_{max}\frac{3R^2}{16} \tag{49}$$

Substituting the values of C_1 *and* C_2 in equation (48), we have

$$t = \frac{1}{\alpha}\frac{\partial t}{\partial x}u_{max}\left(\frac{r^2}{4}+\frac{r^4}{16R^2}\right) + \left[t_s - \frac{1}{\alpha}\frac{\partial t}{\partial x}u_{max}\frac{3R^2}{16}\right] \tag{50}$$

now, with introduction of surface roughness in the above equation, we have

$$t_s - t = \frac{u_{max}}{\alpha}.\frac{\partial t}{\partial x}\left[\frac{3R^2}{16}-\frac{r^2}{4}+\frac{r^4}{16R^2}\right]R_\nabla \tag{51}$$

The above equation indicates the differences between the surface and porous medium temperatures which may contribute in the detachment of fine particles. At next, we will derive an equation for heat transfer coefficient that is total heat energy carried by the fluid influx.

This can be stated as the ratio of flux of enthalpy in pore chamber to the mass flow product and fluid specific heat.

Therefore, we have

$$t_b = \frac{\int_0^R \rho(R_\nabla.dr)uc_p t}{\int_0^R \rho(R_\nabla.dr)uc_p} \tag{52}$$

For an incompressible fluid influx having constant density and specific heat

$$t_b = \frac{\int_0^R utR_\nabla dr}{\int_0^R urR_\nabla dr} \tag{53}$$

The mean mass flow velocity ($\overline{u}$) in porous media is also known as bulk mean velocity can be calculated from the following definition:

$$\overline{u} = \frac{1}{R_\nabla R^2}\int_0^R R_\nabla.dr.u \tag{54}$$

$$\overline{u} = \frac{2}{R^2}\int_0^R ur.dr \tag{55}$$

Substituting this value of u in equation (55), we get

$$t_b = \frac{2}{\overline{u}R^2}\int_0^R utr.dr \tag{56}$$

Substituting the u value from velocity distribution and average velocity flow equation ($\overline{u} = \frac{u_{max}}{2}$) and that of t from equation (56), we get

$$t_b = \frac{2}{\overline{u}R^2}\int_0^R 2\overline{u}\left[1-\frac{r^2}{R^2}\right]\left[t_s - \frac{u_{max}}{\alpha}.\frac{\partial t}{\partial x}\left\{\frac{3R^2}{16}-\frac{r^2}{4}+\frac{r^4}{16R^2}\right\}\right]rdr \tag{57}$$

$$= \frac{4}{R^2}\int_0^R\left[T_s\left[1-\frac{r^2}{R^2}\right] - \frac{u_{max}}{\alpha}.\frac{\partial t}{\partial x}\left\{\frac{3R^2r}{16}-\frac{7r^2}{16}+\frac{5r^5}{16R^2}-\frac{r^7}{16R^4}\right\}dr\right]$$

$$= \frac{4}{R^2}\left[T_s\left(r-\frac{r^3}{R^2}\right) - \frac{u_{max}}{\alpha}.\frac{\partial t}{\partial x}\left\{\frac{3R^2r}{16}-\frac{7r^3}{16}+\frac{5r^5}{16R^2}-\frac{r^7}{16R^4}\right\}dr\right]$$

$$= \frac{4}{R^2}\left[T_s\left\{r - \frac{r^3}{R^2}\right\}\right]_0^R - \frac{4u_{max}}{\alpha R^2}.\frac{\partial t}{\partial x}\left[\frac{3R^2r^2}{32} - \frac{7r^4}{64} + \frac{5r^6}{96R^2} - \frac{r^8}{128R^4}\right]_0^R$$

$$= \frac{4}{R^2}\left[T_s\left\{\frac{R^2}{2} - \frac{R^4}{4}\right\}\right]^R - \frac{4u_{max}}{\alpha R^2}.\frac{\partial t}{\partial x}\left[\frac{3R^4}{32} - \frac{7R^4}{64} + \frac{5R^6}{96} - \frac{R^8}{128}\right]$$

$$= \frac{4}{R^2}\left(T_s \times \frac{R^2}{4}\right) - \frac{4u_{max}}{\alpha R^2}.\frac{\partial t}{\partial x} \times \frac{11}{96}R^4$$

$$t_b = T_s - \frac{11}{96}\frac{u_{max}}{\alpha}R^2\frac{\partial t}{\partial x} \tag{58}$$

Therefore, with an introduction of surface roughness the heat transfer coefficient can be calculated from the below expression:

$$h_\Omega = \frac{Q}{R_\nabla\,(t_s - t_b)} \tag{59}$$

The rate of heat generation in porous media per unit volume with radius of pore chamber R is given by

$$Q_g = a + br^2 \tag{60}$$

where, a and b are the any points on the radius of pore mixing chamber. The porous rock is undergoing heat transfer with a medium coefficient M. Now we can find the steady state temperature distribution on the porous surface.

The controlling differential equation is given by

$$\frac{d}{dr}\left(r.\frac{dt}{dr}\right) + \frac{Q_g}{K}.r = 0 \tag{61}$$

Substituting the value of Q_g, we have

$$\frac{d}{dr}\left(r.\frac{dt}{dr}\right) + \frac{r}{K}\left(a + br^2\right) = 0 \tag{62}$$

Integrating the above equation, we get

$$r\frac{d}{dr} + \frac{1}{K}\left(\frac{ar^2}{2} + \frac{br^4}{4}\right) = C_1 \tag{63}$$

$$\frac{dt}{dr} + \frac{1}{K}\left(\frac{ar}{2} + \frac{br^3}{4}\right) = \frac{C_1}{r}$$

By integrating again, we get

$$t + \frac{1}{K}\left[\frac{ar^2}{2} + \frac{br^4}{16}\right] = C_1\,\ln(r) + C_2 \tag{64}$$

Where C_1, C_2 = constants of integration

The boundary conditions for finding C_1 *and* C_2 are:

At r = 0 $\frac{dt}{dr} = 0$ since $C_1 = 0$.

Therefore,

$$\frac{dt}{dr} + \frac{1}{K}\left(\frac{ar}{2} + \frac{br^3}{4}\right) = 0 \tag{65}$$

and

$$t + \frac{1}{K}\left[\frac{ar^2}{2} + \frac{br^4}{16}\right] = C_2 \tag{66}$$

Now, $(\textit{heat conducted})_{r=R} = (\textit{heat convected})_{r=R}$.

$$\left[-KR_\nabla.\left(\frac{dt}{dr}\right)\right]_{r=R} = [M.R_\nabla(t - t_a)]_{r=R} \tag{67}$$

Substituting the values from equations (65) and (66) for $\frac{dt}{dr}$ and t in the above equation for r = R, we get

$$-K\left[-\frac{1}{K}\left(\frac{ar}{2} + \frac{br^3}{4}\right)\right] = M\left[C_2 - \frac{1}{K}\left(\frac{ar^2}{2} + \frac{br^4}{16}\right) - t_a\right] \tag{68}$$

Therefore,

$$\frac{R}{2M}\left[a + \frac{bR^2}{2}\right] = C_2 - \frac{R^2}{4K}\left[a + \frac{bR^2}{2}\right] - t_a \tag{69}$$

$$C_2 = t_a + \frac{R}{2M}\left[a + \frac{bR^2}{2}\right] + \frac{R^2}{4K}\left[a + \frac{bR^2}{2}\right] \tag{70}$$

Now, substituting this value in equation (66), we obtain

$$t + \frac{R^2}{4K}\left[a + \frac{bR^2}{4}\right] = t_a + \frac{R}{2M}\left[a + \frac{bR^2}{2}\right] + \frac{R^2}{4K}\left[a + \frac{bR^2}{4}\right] \tag{71}$$

Therefore, by introducing a roughness factor, we get

$$t - t_a = \frac{R}{2M}\left[a + \frac{bR^2}{4}\right] + \left[\frac{aR^2}{4K} + \frac{bR^4}{16K}\right] - \left[\frac{ar^2}{4K} + \frac{br^4}{16K}\right] \times R_\nabla \tag{72}$$

Or,

$$t - t_a = \frac{R}{2M}\left[a + \frac{bR^2}{4}\right] + \frac{aR^2}{4K}\left[1 - \left(\frac{r}{R}\right)^2\right] + \frac{bR^4}{16K}\left[1 - \left(\frac{r}{R}\right)^4\right] \times R_\nabla \tag{73}$$

The above equation indicates the temperature distribution due to heat generation within the porous medium. Finally, we can see the heat development in porous medium due to the presence of irregular rock surface roughness. Now, let two ordinates have radii r_1 and r_2 respectively. That is developing heat steadily, Q_d per unit volume per unit time. The heat conductivity of porous media with surface roughness is given by:

$$K = K_0R_\nabla(1 + \beta t) \tag{74}$$

Heat generation rate between $r = r_1$ and $r =$ $r =$ *heat conducted at* $r = r$.

$$(Q_d)_r = Q_dR_\nabla(r^2 - r_1^2) \times 1$$

$$= -K_0R_\nabla(1 + \beta t) \times 1 \times \frac{dt}{dr} \tag{75}$$

1 in the equation indicates the unit length of the rough porous surface.

$$\left(\frac{(r^2 - r_1^2)}{r}\right)\frac{Q_d}{2K_0}dr = -(1 + \beta t)dt$$

$$-\left(r - \frac{r_1^2}{r}\right)\frac{Q_d}{2K_0}dr = -(1 + \beta t)dt \tag{76}$$

Integrating both sides, we have

$$\int(1 + \beta t)dt = -\frac{Q_d}{2K_0}\int\left(r - \frac{r_1^2}{r}\right)dr \tag{77}$$

Or,

$$t + \beta\frac{t^2}{2} = -\frac{Q_d}{2K_0}\left[\frac{r^2}{2} - r_1^2\ln(r_2)\right] + C \tag{78}$$

Using boundary condition (for finding the constant C), at r = r, t = t_w, we have

$$C = t_w + \frac{\beta}{2}{t_w}^2 + \frac{Q_d}{2K_0}\left[\frac{r^2}{2} - r_1^2\ln(r_2)\right] \tag{79}$$

Substituting the value of C in equation (78), we have

$$t + \frac{\beta}{2}t^2 = -\frac{Q_d}{2K_0}\left[\frac{r^2}{2} - r_1^2\ln(r_2)\right] + t_w + \frac{\beta}{2}{t_w}^2 + \frac{Q_d}{2K_0}\left[\frac{r^2}{2} - r_1^2\ln(r_2)\right] \tag{80}$$

$$\frac{\beta}{2}t^2 + t + \frac{Q_d}{2K_0}\left[\frac{r^2}{2} - r_1^2\ln(r_2)\right] - t_w - \frac{\beta}{2}{t_w}^2 - \frac{Q_d}{2K_0}\left[\frac{r^2}{2} - r_1^2\ln(r_2)\right]$$

$$\frac{\beta}{2}t^2 + t - \left[\frac{\beta}{2}{t_w}^2 + t_w + \frac{Q_d}{2K_0}\left\{\frac{r_2^2 - r^2}{2} - r_1^2 \ln\left(r_2/r\right)\right\}\right] = 0$$

$$t = \frac{-1 + \sqrt{1 + 4 \times \frac{\beta}{2}\left[\frac{\beta}{2}{t_w}^2 + t_w + \frac{Q_d}{2K_0}\left\{\frac{r_2^2 - r^2}{2} - r_1^2 \ln\left(r_2/r\right)\right\}\right]}}{\beta}$$

$$t = -\frac{1}{\beta}1 + \sqrt{\left\{\left(\frac{1}{\beta}\right)^2 + {t_w}^2 + \frac{2}{\beta}t_w\right\} + \frac{2}{\beta}\frac{Q_d}{2K_0}\left\{\frac{r_2^2 - r^2}{2} - r_1^2 \ln\left(r_2/r\right)\right\}}$$

$$= -\frac{1}{\beta} + \sqrt{\left(\frac{1}{\beta} + t_w\right)^2 - \frac{Q_d}{\beta K_0}\left[\frac{r_2^2}{2} + r_1^2 \ln\left(r_2/r\right) - \frac{r_2^2}{2}\right]} \quad (81)$$

Finally, with an introduction of roughness factor R_∇.

$$t = -\frac{1}{\beta} + \sqrt{\left(\frac{1}{\beta} + t_w\right)^2 - \frac{Q_d r_1^2}{2\beta K_0}\left[\left(\frac{r}{r_1}\right)^2 + 2\,ln\left(r_2/r\right) - \left(\frac{r_2^2}{2}\right)^2\right]} \times R_\nabla \quad (82)$$

Therefore, the above equation expresses the heat generation within the porous surface with roughness factor existence. Altogether these factors dominate the fines migration and permeability reduction mechanism. Ultimately, this process will deteriorate the well productivity. It should be noted that the soaring reservoir temperature have a significant impact on the critical retained particle concentration and well impedance index profile. Also, the retained particle concentration decreases with increasing temperature at even with minimum velocity. Furthermore, the well impedance (denoted as J) aggravates with rising temperature. Therefore, modelling demonstrates that the varying formation and well temperatures will lead to formation damage. In addition, it can be observed from the modelling that the rock surface morphology plays an important role in wettability of fine particles in subsurface environment.

This modelling will help us to explore the relationship between rock surface roughness-fluid-particle wettability and also relationship between rock texture-fine particle wettability-fluid flow velocity. Thus, this semi-analytical modelling elucidated the importance of the role of geologic fabrics on fluid flow behaviour and fines drift. The developed surface thermodynamic analytical model indicates that the fines slow mobilization over porous rock surface is initially due to temperature distribution and rock surface roughness. Fabric theory concept was applied to this problem and from modelling, it was noted that rock texture and roughness will decline the fluid flow velocity and suspension flow (particle transport). Furthermore, the variation in the thermal conductivity of irregular rock surface roughness is capable to alter the wettability of fine particle. Even, a microscale surface roughness will change the particle wettability (Kumar and Prabhu, 2007). Totally, these factors contribute in the liberation and slow mobilization of fines in porous media. This entire analytical modelling derivation has been optimized and the reader is advised to see the appendix section for full mathematical derivation.

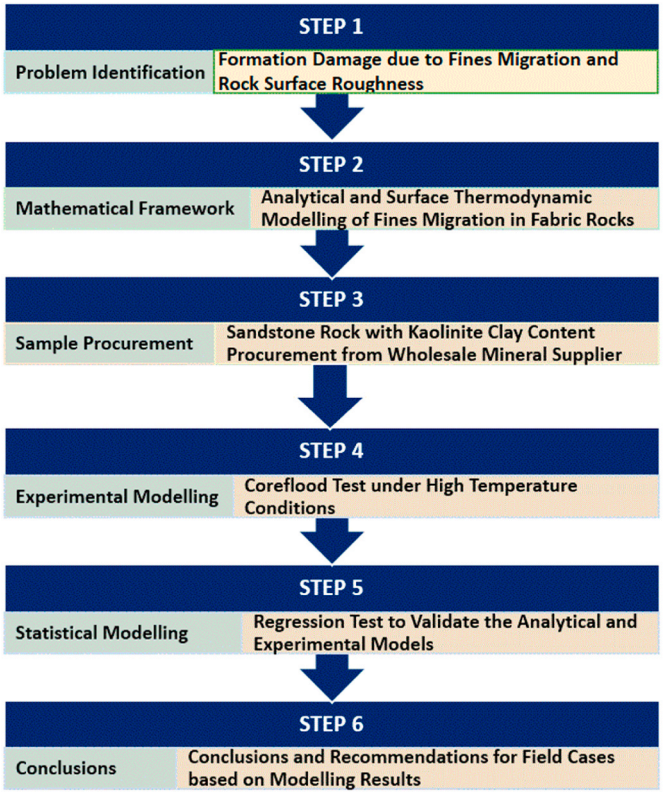

Fig. 3. Research flowchart.

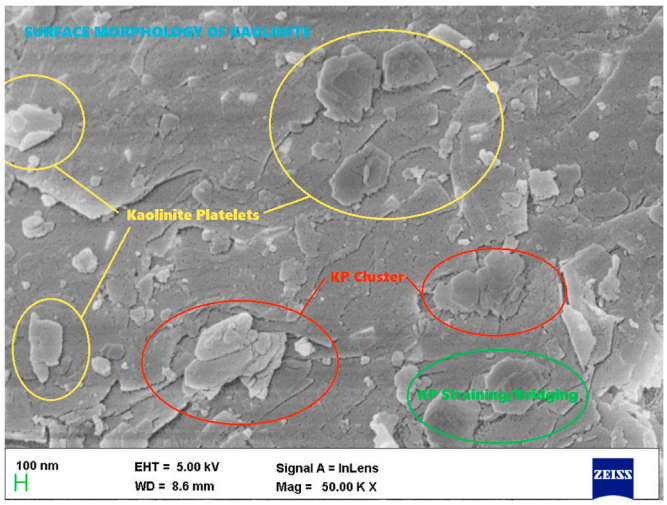

Fig. 4. Surface Morphology of Kaolinite Clay Mineral under 100 nm Magnification. For enlarged view of image, the reader is advised to see the appendix.

3. Materials and methods

This section presents the materials and methods that were employed in this investigation. Actually, two sets of coreflood flow test experiments were performed at the temperatures 50 °C (Normal Temperature, NT) and 150 °C (High Temperature, HT).

3.1. Sample preparation

This research work consists of six major steps such as problem identification, mathematical framework, sample procurement, experimental analysis, statistical modelling, and conclusion, and recommendations, which is presented as flow chart in Fig. 3.

Fig. 4 shows the scanning election microscopic image of kaolinite clay surface morphology under 100 nm magnification and the clay mesh size is 200 (74 μm). So, a sandstone core with 36 wt% kaolinite clay content was taken for the tests and the core is having 10 cm diameter and a length of 30 cm. The sandstone core is having 28% porosity and permeability 200 mD. The core holder is exclusively customized for this coreflood test and this sandstone was procured from a wholesale mineral supplier. The origin of this sandstone rock is from Cauvery Basin, Tamil Nadu, South East India. Actually, Cauvery basin is a peri-cratonic fault rift basin with significant gas reserves, and the basin is highly kaolinitic (Mukherjee, 2015a, 2015b; Mazumder et al., 2019), which means the reservoir is dominated by the kaolinite clay in which the rock formation contains 91.04% deposits of kaolinite clay mineral (Murthy et al., 1950;

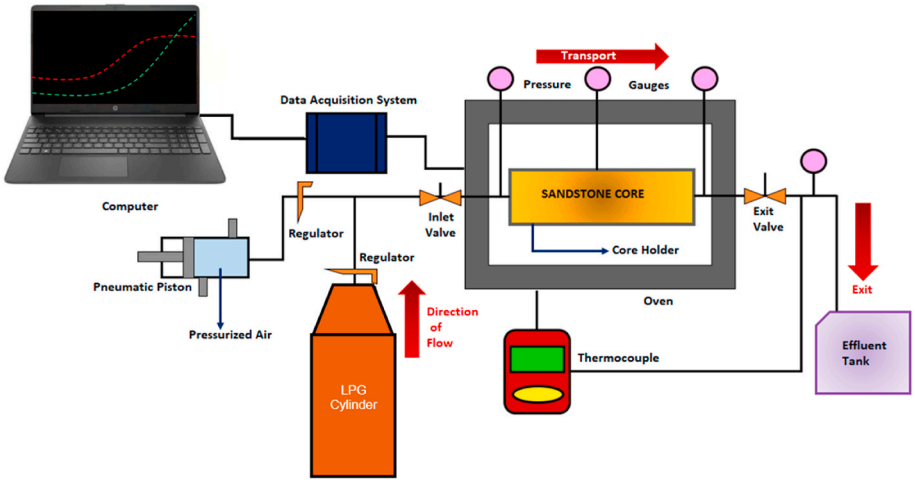

Fig. 5. Coreflood Experimental Setup. For enlarged view of image, the reader is advised to see the appendix.

Sinha and Guha, 1990) and highly susceptible to reservoir formation damage (permeability deterioration) and well productivity decline (Kanimozhi et al., 2021).

3.2. Coreflood setup

The coreflood experimental design and procedure was deployed and conducted in accordance with the methodology guided by the literatures Kanimozhi et al. (2020) and Pranesh et al. (2019). Fig. 5 shows a schematic diagram of the coreflood test setup. It can be seen from the figure that the sandstone core is placed in a stainless steel cylindrical core holder and in turn placed inside the oven. The oven is attached with a thermocouple and three pressure gauges (for measuring the pressure difference across the core). One pressure gauge is connected to the inlet and outlet flow lines of the core centre and another two are connected to the inlet and outlet flow lines of the core. One side of the core holder has provisions for pneumatic piston pump (for pressure exertion) and suspension flow. On this same side LPG cylinder is attached and overall these components are connected to the core oven system. Other side of the core oven apparatus has the provision (exit line) for effluent tank (for collecting the suspension-colloids). The flow lines are provided with ball valves and the whole core-oven thermal system is connected to the data acquisition system and subsequently, connected to the computer.

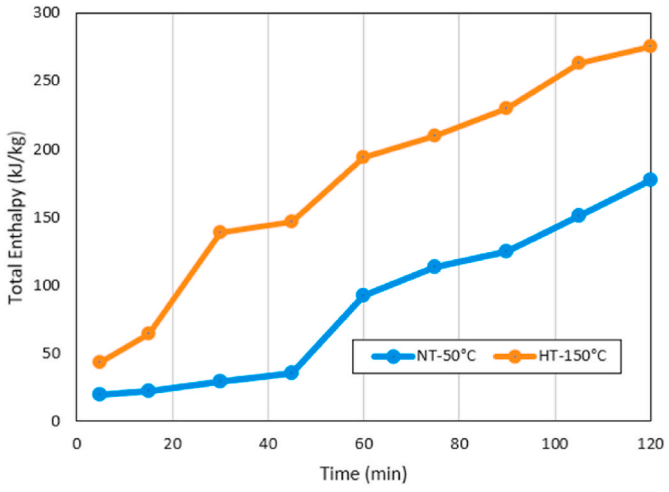

Fig. 6. Variation of enthalpy release with respect to increasing time. For enlarged view of image, the reader is advised to see the appendix.

3.3. Coreflood test procedure

Following is the coreflood test procedure:

a) Firstly, LPG cylinder is released and a mass of 25 kg gas at normal temperature (50 °C) is injected in the permeable sandstone rock core. Subsequently, the mobilized kaolinite clay fines-gas suspension (adsorbed on the fines) is collected in the effluent collector tank (containing cold water).
b) The previous procedure **a)** is continued for higher temperature (150 °C).
c) Then, samples in the effluent were dried and sent to microstructural tests for analysing the morphology and orientation of kaolinite fine particle that has potentially damaged the sandstone permeability and gas recovery, and decline as well.
d) Furthermore, SPSS statistical modelling was performed for model validation. It should be noted that **c)** and **d)** steps are not part of coreflood experimental test and they are individually conducted in Field Emission Scanning Electron Microscope (FESEM) machine and Statistical Package for Social Science (SPSS) software.

4. Results and discussions

This section explores the results that were acquired in the experimentation. A critical analysis and serious discussions were made. Fig. 6 shows the total enthalpy release with respect to increasing time. The total enthalpy is the summation of enthalpy of permeable reservoir rocks and transporting fluid (Kanimozhi et al., 2020). Already it was mentioned that enthalpy indicates the quantity of heat release or heat content (thermal potential). It can be seen from Fig. 4 that for both normal (50 °C) and high (150 °C) temperatures the total enthalpy of the sandstone core gradually rises in which the intensity of HT is higher. Actually, gas flow rate in the porous rocks increases the reservoir temperature and subsequently, releases the in-situ fines to transport in the permeable medium, as given by the following modified equations (Senthil et al., 2019).

$$U_2 = \sqrt{S_g} + U_1 \tag{83}$$

$$\eta_{\varphi R} = \frac{W_R}{Q_1} \tag{84}$$

Where, U_2 *is the final velocity of gas in porous media* (*leaving the cappillary tube to enter another mixing chamber*, U_2 *is the initial velcoity of in porous media* (*entering the cappillary tube from mixing chamber*, S_g *is the gas saturation*, $\eta_{\varphi R}$ *is thermal efficieny of porous media with respect to*

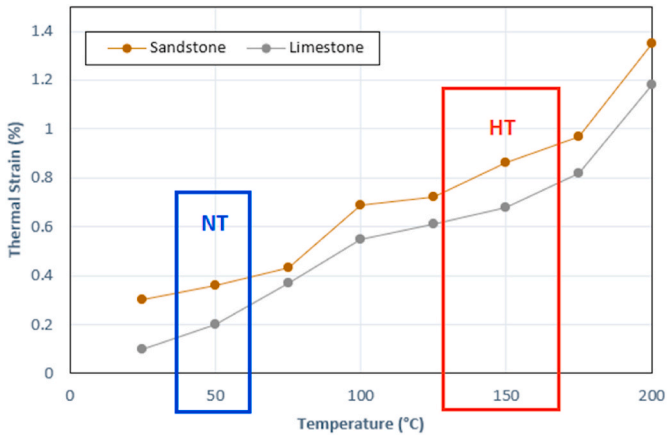

Fig. 7. Variation of thermal strain with respect to increasing temperature. For enlarged view of image, the reader is advised to see the appendix.

radiation, W_R is the network done to transport the natural reservoir fines, and, Q_1 is the heat transfer to porous media..

Chequer and Bedrikovetsky (2019), You et al. (2014), and Schembre and Kovscek (2005), reported that during elevated reservoir temperature the fines are detached from rock surface due to the decline of electrostatic and gravitational forces combined and migrate in the porous interspace. This phenomenon is mainly attributed to heat transfer (Kanimozhi et al., 2021; Pranesh and Ravikumar 2019) and moreover, under fines detachment there is an entropy production and new appearance of surface energy, which gives the space for productive flow of kaolinite clay mineral fines and the entropy is governed by the high temperature and pressure in the porous rocks (Kanimozhi et al., 2019a).

The mass flow rate and velocity of fluid flow in the high temperature reservoir produces thermal dispersion (Jiang and Ren, 2001) and in turn becomes a heat transfer fluid. Furthermore, heat capacity ratio in the porous media leads to an oscillatory flow (Di Meglio et al., 2021) of reservoir fluids and particles. In this context-oscillatory flow is the forced vibrations in the porous media due to inertial and drag forces that stimulates the sweep efficiency of the reservoir fluids (Rajkumar et al., 2020; Zeinijahromi et al., 2012) and loose the momentum of fine particles in porous rock (Kampel, 2007) due to collision with pore walls. Therefore, rock and fluid enthalpy content and release quantification are essential in order to estimate the mass flow rate of reservoir fluids and formation damage (fines migration and other phenomenon, for example geochemical leaching) predictions.

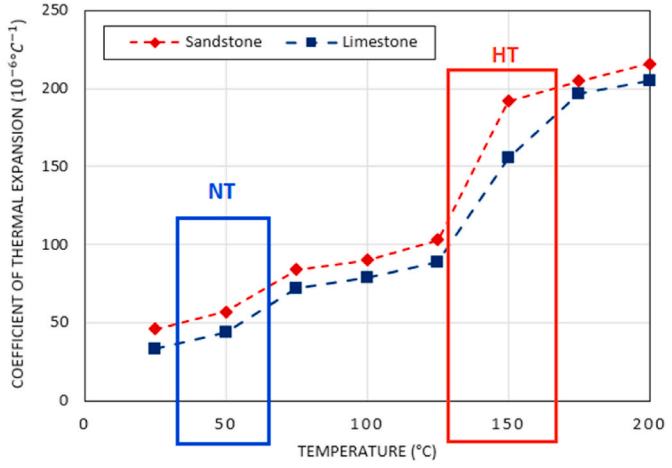

Fig. 8. Variation of CTE with respect to increasing time. For enlarged view of image, the reader is advised to see the appendix.

Fig. 7 shows the thermal strain variation with respect to increasing temperature for both sandstone and limestone. As previously discussed about rock enthalpy that enhancing mass flow rate and velocity of reservoir fluids increases the reservoir temperature and consequently, leads to thermal stress, which in turn cause non-linear elastic deformations (Ehlers, 2018). Generally, reservoir is subjected to stress (σ) and strain (ε) regardless of temperature, but in reservoir engineering σ *and* ε is the function of pressure (Zoback, 2010). It can be seen for the figure that the thermal strain for sandstone and limestone varies linearly and the sandstone rock core thermal strain were found to be higher than the limestone. It is obvious that under soaring temperature sandstone usually undergo a deformation, but carbonate rocks endure a thermo-chemical reaction (Mahalingam et al., 2019). The thermal strain during 50 °C normal temperature (NT) and 150 °C higher temperature (HT) was recorded to be 0.36% and 0.86% for sandstone. While, the carbonate rock limestone accounts for 0.2% and 0.68% at NT and HT. Furthermore, thermal strain is influenced by volumetric strain, effective stress coefficients, Klinkenberg effect on the gas flow permeability in sandstone (Nolte et al., 2021). The thermal stress and strain equation as a function of temperature is given as below:

$$\sigma(t) = \alpha_0 . T_0 . E \tag{85}$$

Where, $\sigma(t)$ *is the thermal stress (function of temperature),* α_0 *is the coefficient of linear expansion* T_0 *is the rise in temperature, and* E *is Young's Modulus..*

Fig. 8 shows the variation of Coefficient of Thermal Expansion (CTE) with respect to increasing time. Actually, equation (85) presents the thermal stress-strain for a material as a function of increasing temperature. This equation could be further extended to equation (86), considering elastic deformation.

$$\sigma(t) = \frac{(\alpha . T . \triangle L - \delta)}{L} \times E \tag{86}$$

Where, $\triangle L$ *is the change in the length of the rock core and* δ *is the coeffc ienct of deformation.*

However, the reservoir is subjected to tensile stress and subsequently, leading to thermal expansion is govern by the following equations:

$$e(t)_1 = \frac{\sigma_1}{E} - \mu\frac{\sigma_2}{E} - \mu\frac{\sigma_3}{E} \quad \text{For X – Axis} \tag{87}$$

$$e(t)_2 = \frac{\sigma_2}{E} - \mu\frac{\sigma_3}{E} - \mu\frac{\sigma_1}{E} \quad \text{For Y – Axis} \tag{88}$$

$$e(t)_3 = \frac{\sigma_3}{E} - \mu\frac{\sigma_1}{E} - \mu\frac{\sigma_2}{E} \quad \text{For Z – Axis} \tag{89}$$

It can be seen from Fig. 8 that CTE varies linearly, also called thermal

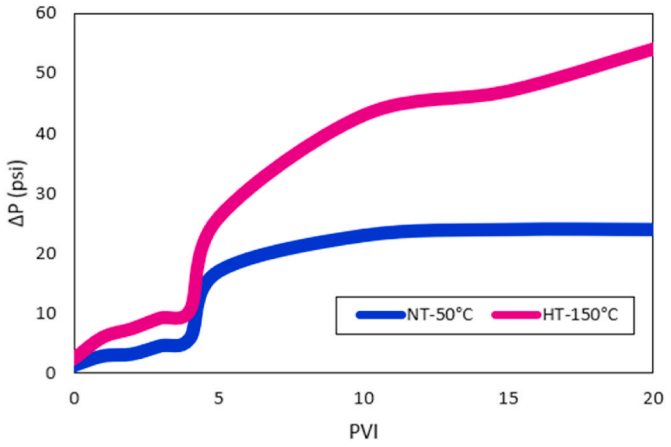

Fig. 9. Pressure variation with respect to increasing pore volume injection. For enlarged view of image, the reader is advised to see the appendix.

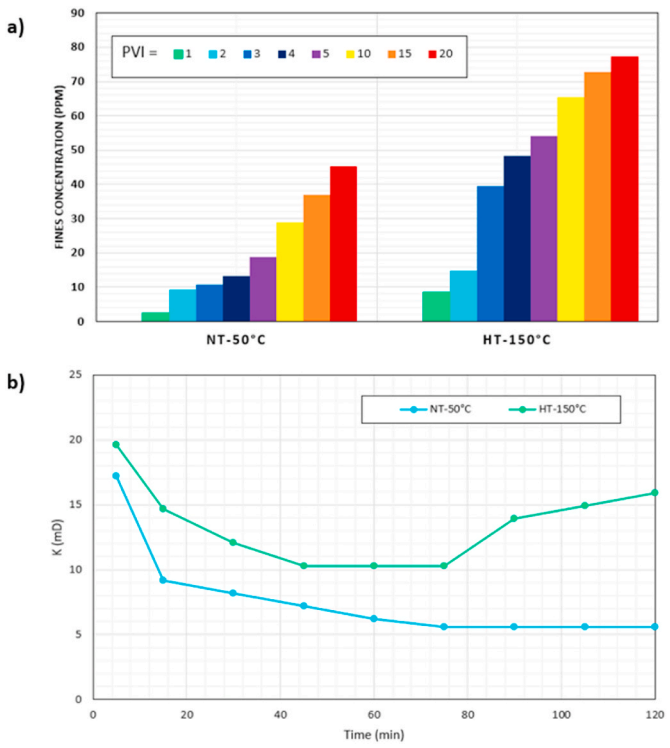

Fig. 10. A) Fines concentration with respect to increasing pore volume injection, b) Permeability variation with respect to increasing time. For enlarged view of image, the reader is advised to see the appendix.

linear expansion (TLE) for sandstone and limestone rock core. The TLE could be measured using the following equation:

$$\delta L = L_0.\alpha_t.(T_f - T_i) \tag{90}$$

Where, *is the change in length*, L_0 *is the original length*, α_t *is the coefficient of thermal expansion* T_f *is final temperature and* T_i *is initial or reference temperature*..

It is noted that for sandstone core the CTE at NT and HT were found to be 57 $(10^{-6^\circ}C^{-1})$ and 192 $(10^{-6^\circ}C^{-1})$, and for limestone it is 44 $(10^{-6^\circ}C^{-1})$ and 156 $(10^{-6^\circ}C^{-1})$. Even in this case the thermal expansion coefficient for sandstone is apparently higher than the carbonate, which is an indication for elongated pore spaces, which enables effective transport of gas and particles in the porous media. Khalili et al. (2010), stated that coefficient of thermal expansion has no impacts on porosity and voids of porous media, but in a recent study it was demonstrated that under the state of local thermal non-equilibrium (LTNE), increase in bulk volumetric CTE of porous media decreases the stress and, decrease the pore-pressure during increase in the fluid mobility ratio, and, due to the LTNE effects, the solid temperature (rock) is greater than the pore fluid (Li et al., 2022). Exponential growth in CTE at 125 °C for both sandstone and limestone rock cores. Moreover, it was revealed in Figs. 5 and 6 that there were no signs of stabilization, but yield strength at 150 °C. Therefore, it is inferred that CTE is the positive indication that the fluid and particles can divert their path for improved recovery. Hence, the knowledge and experimental investigation is absolutely necessary in order to model and forecast the fines intrusion on rock permeability and enhanced fluid recovery. Moreover, it was revealed that porous materials under LTNE state, enthalpy, temperature (surface heat transfer), and velocity dictate the fluid saturation and mass transfer in porous media (Liu et al., 2022). Fig. 9 shows the variation of pressure with respect to increasing pore volume injection. It can be seen from the figure that at NT50 °C the pressure varies linearly and then rises to certain level and then it underwent a stabilization. It indicates that the fines have started to migrate and plugged the pore-throats. It is a usual and frequent phenomenon that the pressure gets to stabilize and drop during coreflood test, which is widely reported in the literatures (Haasan et al., 2022; Kanimozhi et al., 2020; Yang et al., 2019; Chequer et al., 2018; Russell et al., 2018; Vaz et al., 2017; Kanimozhi et al., 2019a; Mahalingam et al., 2019). In the case of HT150 °C the pressure initially behaves as NT, but tends to an exponential rise and then increases steadily and it is noted that there is no sign of stabilization and even in the initial conditions the HT150 °C case was found to be higher than the NT. This behaviour is mainly attributed to the surface roughness of the pore surface, which during the gas flow in the rock or fabrics (rock teeth) will elevate the temperature of the porous rocks. Rough grains initiate the bulk compressibility of reservoir fluid and have tremendous impact on the rock pressure (Wang et al., 2020), and because of thermal stress-strain the sandstone rock core has underwent a slight deformation, which is explained in Fig. 6 and due to these impacts the strain energy in the porous rock has been released, which subsequently increased the rock pressure, mathematically mentioned as below:

$$\varepsilon_e(t) = \frac{P}{A}\left(1 + \sqrt{1 + \frac{2AER_\nabla}{P.L}}\right) \tag{91}$$

Where, $\varepsilon_e(t)$ *is the strain energy as a function of temperature*, P *is load*, A *is area*, L *is length*, E *is young's modulus, and* R_∇ *is surface roughness coefficient*. Thus, surface roughness of grain and rock surface have serious repercussions on the porous media pressure and its network (Bagrezaie et al., 2022).

Fig. 10 a) shows the variation of fines concentration with respect to increasing pore volume injection. Satisfactory production of kaolinite fines was observed in NT50 °C initially the fines concentration was recorded to be 2.2 ppm at 1 PVI and gradually rose to 18.55 ppm at 5 PVI and then the production was sluggish and linear and finally climbing to 45.19 ppm at 20 PVI. Lesser fines production is a sign and for fines straining in the pore-throats and between the rock fabrics (teeth). Moreover, Borazjani and Bedrikovetsky (2017) mentioned that for small retained concentrations in a particular reservoir cross section, the retained concentrations are proportional to the mass of suspended particles. Also, during single-phase flow the suspended and retained particles maximum penetration distance are same and equal that ratio. It is observed that concentration of kaolinite fines surges at each injection pore volume level at HT150 °C. Aggressive growth in the kaolinite fines production was noted between 1 PVI and 5 PVI and gradually rises to

Table 2
Physical properties of produced suspensions.

Injection Parameter (PVI)	Temperature (°C)	Fluid Phase State	Electrical Conductivity ($\mu S/cm$)	Thermal Conductivity ($W/m-K$)	Zeta Potential (mV)
5	50	Normal	138	1.2	+30
10	50	Normal	146	1.4	+16
15	50	Normal	159	1.5	+12
20	50	Normal	172	1.8	+5
5	150	Heat Transfer Fluid	196	3.4	+54
10	150	Heat Transfer Fluid	211	4.1	+44
15	150	Heat Transfer Fluid	228	4.6	+42
20	150	Heat Transfer Fluid	247	5.5	+33

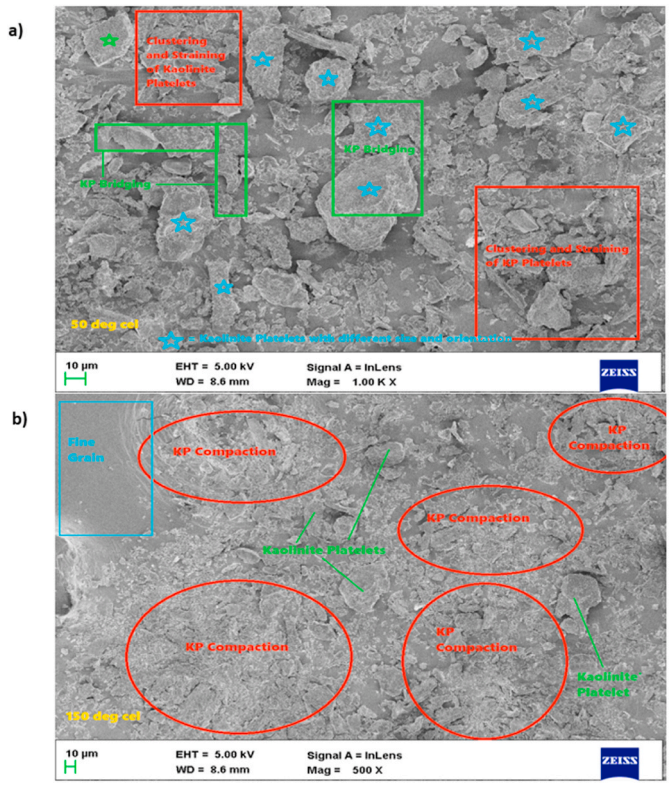

Fig. 11. Microstructural image of the produced suspensions, a) 50 °C, b) 150 °C. For enlarged view of image, the reader is advised to see the appendix.

77.28 ppm at 20 PVI. This phenomenon is mainly due to production velocity (of both gas and particle), internal heat transfer, and surface heterogeneity, which overall weakens the electrostatic and gravitational forces and give acceleration to lift and drag forces to detach and transport in the permeable rock (Kanimozhi et al., 2021; Pranesh et al., 2019). But, in this case huge amount of fines concentration production is evidence for more clearance space in the porous sandstone core and also, kaolinite fines were deposited between the rock teeth fabrics and thereby creating new surface energy for rapid flow of gas and particles towards the core end (production well in a field scenario). However, surface roughness promotes particle-wall collision and resulting in energy dissipation (Krull et al., 2021) this statement is evident from our research that fines detachment causes entropy production. Fig. 10 b) shows the variation of permeability with respect to increasing time.

It can be seen from Fig. 10 b) that at NT50 °C experienced a plummet and then gradually declines and finally after 75 min. This is only attributed to fines plugging in pore-throat phenomenon by a process called size exclusion mechanism (Zhang et al., 2018) in which the fine particle size is greater than the pore-throat size where the fines are captured and unable to penetrate further. Even particle and pore shape (geometry) play a crucial role in fines straining (Ting et al., 2021; Yang and Balhoff, 2017). While the NT150 °C case, the permeability began to fall and linear decline and stabilization was observed and then an ascending rise in the permeability was recorded. This breakthrough is due to new surface energy creation, where most of the kaolinite fines concentrations has been retained in the rock fabrics, thanks to the presence of surface roughness factor. New permeable spaces have been created or extended in the rock core and thereby, having more clearance space for gas flow and recovery. Moreover, it was reported that particle elasticity/elastic deformation also influences the reservoir profile control, more specifically the permeability (Chen et al., 2023), and, it was inferred from the literature that clay minerals and gas phase presence is essential in sandstone reservoir for permeability evolution to happen (Al-Yaseri et al., 2017). On the whole, influences of capillarity force, gravity force, breakthrough in fines concentrations dominate the permeability profile of porous rocks (Yang and Bedrikovetsky, 2017; Bagudu et al., 2015). Most importantly, the clay fine particles arrangement-rearrangement-orientation reduce the permeability and provides preferred or new pathways to transport the reservoir fluids (Goldenberg et al., 1993). Table 2 presents the physical properties of produced suspensions.

Fig. 11 shows the microscopic images of produced suspensions at 50 °C (a) and 150 °C (b). In general, the microstructure of fine particle including shape, geometry, orientation, morphology, etc are quantified only by Field Emission Scanning Electron Microscopy (FESEM) technique (Prempeh et al., 2020; Chequer and Bedrikovetsky, 2019; Pranesh et al., 2019; Civan, 2007; Khilar and Fogler, 1998). The received colloidal-suspensions in the effluent tank were dried for hours and then sent to FESEM analysis in order to examine the kaolinite clay fines structure that had potentially impeded the gas flow and destructed the permeability. It can be seen from Fig. 11 a) that at NT150 °C there is an observable appearance of kaolinite platelets or in other words the kaolinite fine particle is having a platelet geometry and apparently different size and orientation of kaolinite platelets (KP) were observed. Furthermore, even at normal reservoir rock temperature the KP bridging, straining, and clustering were detected. This blockage mechanism is attributed to the slow mobilization of fines over the fabric surface, where there is no energy to accelerate the particles to core end and consequently, losing the momentum and finally getting strained and deposited in pore-throats, and overall damaging the permeability. In these cases, detached fines travel near the pore walls and the migrating fines drift speed is lower than the velocity of carrier/permeating fluid (Yang et al., 2016; Oliveira et al., 2014). Most importantly, fines straining in the narrow-pore throats causes a growth in linear skin factor (Bedrikovetsky et al., 2011). Actually, Yang et al. (2016a,b) and Oliveira et al. (2014) examined the slow transport of clay mineral fines in the reservoir rocks during fluid flow. Both examined that fines drift velocity is slower than the carrier fluid flow velocity and there was a significant damage to the permeability and well productivity. Individually, authors observed this phenomenon, but could not be able to give convincing explanation for the slow mobilization of fines in the porous rocks. Thus, our work has filled this research gap by providing explanations (evidences) through experimental demonstrations, analytical cum thermodynamic framework, and statistical modelling. Overall, substantiated the slow movement of fine particles in the porous reservoir rocks.

It can be seen from Fig. 11 b) that there is also a clear appearance of kaolinite platelets at higher reservoir temperature 150 °C. Actually, Chequer et al. (2018) implied that there will be a kaolinite fines mobilization in sand grains that cease the flow in permeable rocks. But, in this case the kaolinite platelets have undergone a compaction over the sand grain as it is evident in the image 12 b) and also, a conspicuous emergence of fine grain. This is mainly attributed to the elevated rock temperature and fluid flow velocity. The kaolinite fines are compacted over the rock surface fabrics (teeth) and filled the teeth spaces and thereby reducing the feasibility of fines plugging and creating new pathways for productive flow of fluid and particles to the core end (in field cases it is wellbore). Literature reporting indicates typically compaction in porous rocks reduces the permeability and gas flow rate (Chen et al., 2020), but in this case we have achieved effective flow of fluid and particles with clay compaction. Actually, in our model compaction happens over the rock fabrics and not on the pore-throat regions. Thus, the microstructural outcomes and analysis proved the positive aspects of kaolinites in fabric sandstones at higher reservoir temperatures. Hence, the retention coefficient is determined by the exponential relationship between the ratio of sand grain and clay size (Won et al., 2021).

Fig. 12 presents the schematic diagram of possible mechanism of kaolinite fines (platelets) induced formation damage and improved recovery. This mechanism and diagram were formulated based on the microstructural images and experimental results, where the circumstantial evidence for kaolinite fines behaviour under NT and HT with

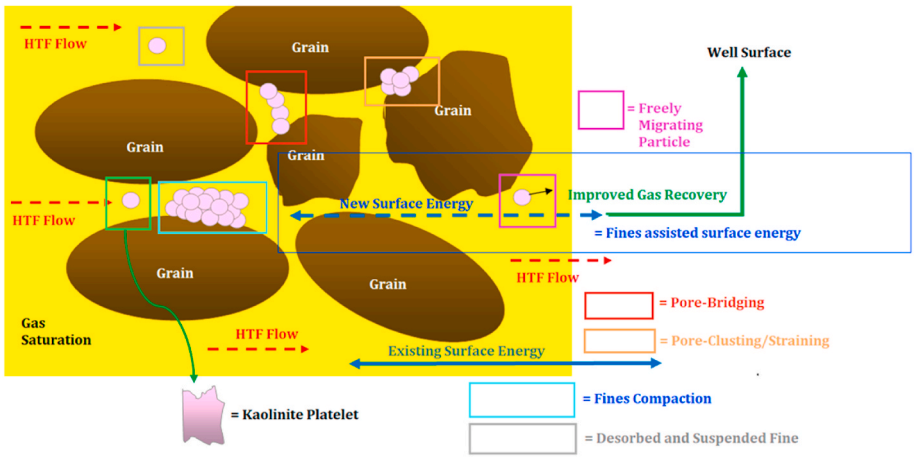

Fig. 12. Proposed mechanism for the occurrence kaolinite fines induced formation damage and improved recovery. For enlarged view of image, the reader is advised to see the appendix.

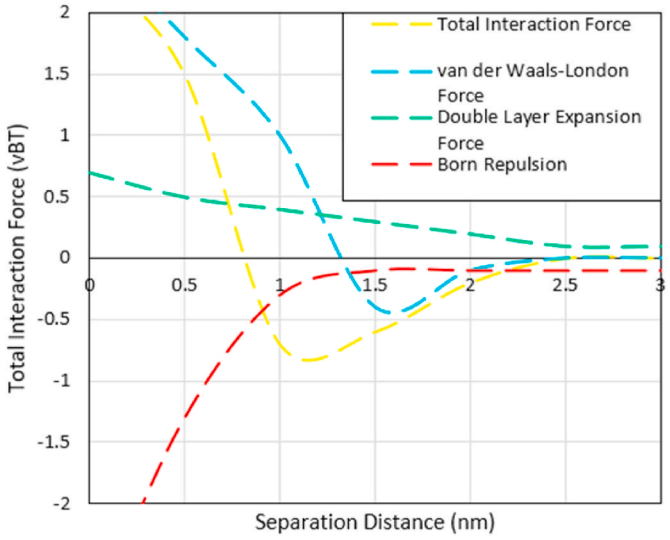

Fig. 13. Electrostatic interaction between kaolinite platelets and fabric sand grain during high enthalpy fluid flow at normal (50 °C) and higher (150 °C) reservoir temperatures. For enlarged view of image, the reader is advised to see the appendix.

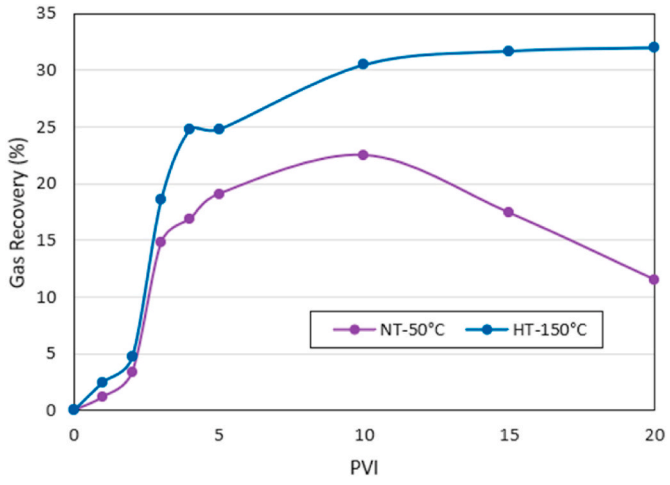

Fig. 14. Gas recovery with respect to increasing pore volume injection. For enlarged view of image, the reader is advised to see the appendix.

surface roughness is stronger in this proposed theory. It can be viewed from the image 11 that the grains are equant and the actual rock matrix is anisotropic. So the experimental and FESEM results reveal that sandstone rock grains having a rough texture and in this penetrative fabric the particle and fluid flow behaviour are weird and abnormal. It can be seen from the proposed theoretical mechanism that kaolinite platelet fines under heat transfer fluid-gas (at 150 °C temperature-flow regime) freely and rapidly mobilize in the porous interspace. Certain amount of fines are strained and clustered in pore-throat and some retained concentration of kaolinite undergo a bridging. During soaring reservoir temperature kaolinite platelets will compact over rock surface fabrics, which creates new surface energy that is clearance space for fluid-particle transport. So, heat transfer fluid-gas (HTF), temperature, surface roughness and gas influx enhanced the rock temperature and created new pore spaces and permeability for efficacious mass transport and recovery of reservoir fluid and particles. Also, the fluid-rock interaction, fluid-particle wettability, temperature, and flow velocity play a vital role in the well flow increment (Isah et al., 2022).

Fig. 13 presents the electrostatic interaction between kaolinite platelets and rough sand grain during high enthalpy fluid flow at NT and HT. It can be seen from the figures that all four curves namely total interaction force (TIF), van der Waals-London force, double layer expansion force, born repulsion force. The overlap of these four curves signals that kaolinite platelets have undergo detachment, migration, re-attachment, straining and plugging in pore-throat and deposited between the rock surface fabrics. These forces contribute in the attraction and repulsion of Kaolinite fines in the porous media. Moreover, kaolinite fines exhibit positive and negative total interaction force, which the fines concentration were retained and strained in the porous rocks. Actually, positive TIF is a repulsion force and negative TIF is attraction forces, which the latter phenomenon is fine particle attachment and reattachment over the rock surface (Xie et al., 2017). Besides, Russell et al. (2017), emphasized that TIF quantification and analysis is vital in order to investigate the kaolinite clay fines transport and retention in the permeable rocks during carrier fluid flow. Therefore, kaolinite fines behaviour in sandstone rock core has been successfully evaluated using DLVO theory.

Fig. 14 presents the gas recovery with respect to increasing pore volume injection for NT and HT temperature regimes. It its apparent from Fig. 14 that under both temperature regimes of 50 °C and 150 °C the gas recovery rate had a slight growth ranging from 1.2% to 19.1% and 2.5%–24.8% from 1 PVI to 5 PVI respectively. Then the gas recovery rate took an exponential rise and the major reasons for this ascending curve is due to combination of several factors such as a temperature, heat transfer, surface roughness, and existence of clay fines, which was

discussed and critically analysed in the previous sections. However, the performance of gas recovery under HT is significantly greater than the NT regime. Surface roughness and thermal diffusivity of sandstone rock (Pranesh et al., 2019) has contributed in this growth. Most importantly, it was mentioned in Fig. 10 that new surface energies were created by kaolinites fines that had compacted over rock fabrics, which paved new path (for fluid-particle transport) and diverted the fluid flow. Actually, the modified surface energy equation is mentioned as below (Kanimozhi et al., 2019b):

$$\nabla(s+\gamma) = -\left[\frac{\partial}{\partial t}(\varphi c+\sigma_a+\sigma_s)+R_\nabla U\frac{\partial c}{\partial t}+\dot{m}\left(\frac{P}{\rho}+\frac{v^2}{2}+gz\right)+\dot{W}\right].k_B \tag{92}$$

where,

$\nabla(s+\gamma)$ *is change in entropy and surface energy in porous rocks*, φc *is critical retained concentration*, $\sigma_a + \sigma_s$ *is concentrations of attached and strained fines*

U *is the flow velocity*, R_∇ *is surface roughness coeffcient*, $\dot{m}$ *is the mass flow rate*, $\frac{P}{\rho}$ *is flow energy*, $\frac{v^2}{2}$ *is kinetic energy*, gz *is potential enegry*, $\dot{W}$ *is work done per second*, *and* k_B *is Boltzmann Constant*

Therefore, equation (91) suggest that entropy production and fines migration is indispensable for the simultaneous achievement of reservoir fluid recovery and formation damage control. Afterwards, the gas recovery rate under NT experienced a sluggish growth and slight stabilization and then underwent a linear decline. This phenomenon mainly attributed to carrier fluid velocity and mass flow rate, in which the fines are carried away in the form of suspensions and strained the pore-throats, resulting is permeability decrease and well productivity loss (Zeinijahromi et al., 2012) and the permeating fluid perturbs the mechanical equilibrium of fines over rock surface (Nguyen et al., 2013). While, in the 150 °C temperature regime, after exponential elevation the gas recovery rate plateaued and showed a linear increase and constant stabilization. Actually, constant stabilization means the rate of gas recovery is monotonous or in other words constant mass recovery is produced irrespective to increasing pore volume injection. This case is due to the new velocity alteration of the carrier fluid, where it can influence the flow pattern and trigger fines plugging (Bedrikovetsky et al., 2012), but it does not mean that formation damage that is fines migration will never occur in high temperature conditions. Most importantly, the presence of rock fabrics has made a significant contribution in the elevation of reservoir temperature that alters the transport of fluid-particle flow velocity pattern in the porous sandstone rock.

Fig. 15 shows the model validation between coefficient of thermal expansion and temperature (a) and gas recovery against pore volume injection (b). Model validation by statistical modelling is required in order to determine the relationship between conditional and response factors (Ajona et al., 2022), and it is usually established by multiple linear regression method (Mateus et al., 2021). Actually, in this work for model validation, we have deployed machine learning based regression modelling (Yun et al., 2022; Ao et al., 2019) to evaluate and validate our models (experimental and analytical models against the regression-R^2) accuracy and reliability. Moreover, multiple linear regression technique examines and estimate the relationship between quantitative dependent and independent variables or in other words it is a statistical method that employ different variables to predict the response variables outcome (Jameel et al., 2016). Therefore, Statistical Package for Social Science (Pandya et al., 2011) abbreviated as SPSS for used to validate our models.

Two parameters coefficient of thermal expansion (CTE) and gas recovery against temperature and pore volume injection (PVI) was taken for modelling, and their average experimental outcome values was fed into the software for processing and analysis. The statistical-machine learning-regression outcomes reveals that there is an excellent and strong agreement between the variables (Fegade et al., 2013) and the plots convergence indicates that the entire model is a good fit with having R^2 values to be 0.9997 and 0.9995, and regarding these terminologies a reader is advised to explore the reference Fegade et al. (2013). In addition, list of frequent usage regression statistical terminologies is

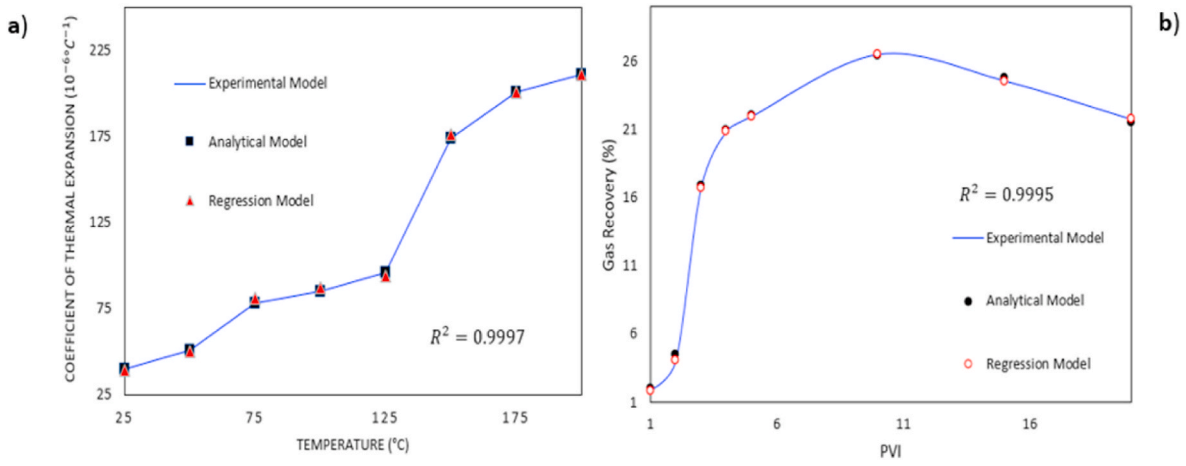

Fig. 15. Model validation: a) Coefficient of Thermal Expansion Vs Temperature, b) Gas recovery Vs Pore Volume Injection. For enlarged view of image, the reader is advised to see the appendix.

presented in appendix II. Even Kanimozhi et al. (2021) and Pranesh et al. (2019), achieved $R^2 = 0.9$ in their similar investigations. Moreover, related to this study, Yu et al. (2021), analysed the sandstone permeability under triaxial stress using multiple linear regression analysis and other machine learning techniques. The authors studied the permeability evolution in tight gas sandstone and applied modelling to estimate and validate the permeability and variation under triaxial stress. Their modelling outcomes reveals that gas bearing tight sandstone reservoirs under triaxial stress has significant impacts on the permeability, often leading to deterioration, whereas the multiple linear regression methods predicted (Fegade et al., 2013) that permeability increased with an increase of pore pressure. Therefore, the authors model accurately predicted the permeability change with respect to external force and subsequently, other machine learning methods have validated the author's model. So likewise in our research investigation, by using this statistical technique, we have achieved our designed outcome and validated the model. To conclude this model can also be extended to onshore and offshore field cases.

5. Conclusions

Reservoir temperature escalation, fines migration, and productivity decline are a syndrome of formation damage and well impairment. Tackling and mitigating fines migration during soaring rock temperate is a great challenge to engineers and researchers. Several studies reported the causes and solutions for reducing the intensity of this problem and also, few work demonstrated the positive aspects of fines migration in which clay particle migration leverage the fluid production to surface. Hence, this paper presented a spotlight on a new sources of fines migration in natural gas reservoirs and insights on productivity enhancement and gas recovery. Overall, a simultaneous processing of gas recovery and formation damage control was achieved. Therefore, based on the experimental and modelling outcomes following conclusions can be established:

- Initially, a surface thermodynamic analytical model was developed for mathematical analysis of fines behaviour under normal and high temperature during high enthalpy gas flow in porous rocks and subsequently, there was a high degree of enthalpy (heat) release in the porous media. This caused sandstone reservoir rock to undergo elongation and deformation, which greatly impacted the transport properties of fluid and particle flow in the porous rock. Specifically, the rock surface roughness (geological fabrics) governs the permeability deterioration and gas recovery.
- Fines plugging in pore-throat area and gas flow over rock teeth (surface roughness) has contributed in the rock core pressure stabilization and escalation. Huge concentration of kaolinite fines was quantified at higher rock temperature. In normal temperature regimes most quantity of fines was carried away by permeating fluid and deposited in pore-throat area, but during HT flow huge mass of fines were deposited between the rock teeth (fabrics). Size exclusion mechanism of particle retention in pore-throat area has contributed in permeability decline at NT, but at HT an initial decline and breakthrough was observed and this is mainly attributed to the role of surface roughness in which kaolinite fines were trapped and new permeable spaces were evolved.
- Microstructural examinations revealed that kaolinite was found to have a platelet geometry and there was an observation of KP undergoing bridging, straining, and clustering. While, at 150 °C the kaolinite underwent a compaction over rock fabric. Total interaction forces reveal that kaolinite-rock attraction and repulsion has occurred, which confirms that kaolinite fines triggered the permeability decline. Exponential growth of gas recovery was achieved at HT150 °C and then it had a linear rise with slow growth, and then it had a constant stabilization that is the recovery is monotonous. It is constant mass of gas is produced regardless of increasing injection of pore volume. ss
- Multiple linear regression was applied to this experimental and analytical modelling for checking and validating the model accuracy and reliability. The modelling results showed a high agreement and valid, where the R^2 values were found to be 0.9997 and 0.9995. Finally, new root cause of fines migration has been successfully identified, which reveals that the rock surface roughness acts as a central role in the detachment and re-attachment of fine particles between rock teeth and increasing the well productivity, thereby overall reducing the formation damage intensity to a considerable level. In our future work, we tend to perform 3D modelling of fabric rock surface distribution and visualization of heat transfer, gas-particle transport over the rough grains and rock teeth in order to study the formation damage and improved recovery.

Credit author statement

B. Kanimozhi: Experimental Setup and Work, Model Prediction, Calculation; P. Rajkumar: Rock Core Examination and Clay Minerals Characterization; S. Mahalingam: Experimental Setup and Work, and Supervision; S. Senthil: Experimental Setup and Work, SEM Interpretation; D.S. Jayalakshmi: SEM Interpretation and Sample Physical Properties Examination; H. Girija Bai: Data Evaluation, Calculation and Analysis; Vivek Thamizhmani: Data Evaluation, Calculation and Analysis; Ramadoss Kesavakumar: Statistical Modelling and Supervision; Venkat Pranesh: Experimental Design, Analytical Modelling, and Wrote the Manuscript.

Declaration of competing interest

The authors declare that they have no known competing financial interests or personal relationships that could have appeared to influence the work reported in this paper.

Data availability

The data that has been used is confidential.

Acknowledgement

This project will not be feasible without technical support and scientific guidance from SIST-Chennai and KCET-Virudhunagar, and their collaboration and MOU with DAWN-CALORIFIC company are greatly acknowledged. Also, especial thanks to Dr. S. Ravikumar, M.E, Ph. D, R&D Head at DAWN-CALORIFIC for the consultation on mass transfer and geomechanics in high temperature gas reservoirs.

Appendix A. Supplementary data

Supplementary data to this article can be found online at https://doi.org/10.1016/j.jgsce.2023.204993.

References

Ajona, M., Vasanthi, P., Vijayan, D.S., 2022. Application of multiple and polynomial regression in the sustainable biodegradation process of crude oil. Sustain. Energy Technol. Assessments 54, 102797.

Al-Yaseri, A., Zhang, Y., Ghasemiziarani, M., Sarmadivaleh, M., Lebedev, M., Roshan, H., Iglauer, S., 2017. Permeability evolution in sandstone due to CO_2 injection. Energy Fuels 31, 12390–12398.

Alshakhs, Mohammed, J., Kovscek, Anthony R., 2016. Understanding the role of brine ionic composition on oil recovery by assessment of wettability from colloidal forces. Adv. Colloid Interface Sci. 233, 126–138.

Ao, Y., Li, H., Zhu, L., Ali, S., Yang, Z., 2019. The linear random forest algorithm and its advantages in machine learning assisted logging regression modeling. J. Petrol. Sci. Eng. 174, 776–789.

Aoyagi, K., Chilingarian, G.V., 1972. Clay minerals in carbonate reservoir rocks and their significance in porosity studies. Sediment. Geol. 8, 241–249.

Argent, J., Torkzaban, S., Hubbard, S., Le, H., Amirianshoja, T., Haghighi, M., 2015. Visualization of micro-particle retention on a heterogeneous surface using micro-models: influence of nanoscale surface roughness. Transport Porous Media 109, 239–253.
Askari, R., Hejazi, S.H., Sahimi, M., 2018. Thermal conduction in deforming isotropic and anisotropic granular porous media with rough grain surface. Transport Porous Media 124, 221–236.
Bagrezaie, M.A., Dabir, B., Rashidi, F., 2022. A novel approach for pore-scale study of fines migration mechanism in porous media. J. Petrol. Sci. Eng. 216, 110761.
Bagudu, U., McDougall, S.R., Mackay, E.J., 2015. Pore-to-Core-Scale network modelling of CO_2 migration in porous media. Transport Porous Media 110, 41–79.
Bedrikovetsky, P., Vaz Jr., A., Machado, F., Zeinijahromi, A., Borazjani, S., 2011. Well productivity decline due to fines migration and production: (Analytical model for the Regime of strained particles accumulation). In: SPE European Formation Damage Conference. Society of Petroleum Engineers, Netherlands.
Bedrikovetsky, P., Zeinijahromi, A., Siqueira, F.D., Furtado, C.A., de Souza, A.L.S., 2012. Particle detachment under velocity alternation during suspension transport in porous media. Transport Porous Media 91, 173–197.
Bernardin, J., Mudawar, I., Walsh, C., Franses, E., 1997. Contact angle temperature dependence for water droplets on practical aluminum surfaces. Int. J. Heat Mass Tran. 40 (5), 1017–1033.
Borazjani, S., Bedrikovetsky, P., 2017. Exact solutions for two-phase colloidal-suspension transport in porous media. Appl. Math. Model. 44, 296–320.
Borazjani, S., Behr, A., Genolet, L., Net, A., V, D., Bedrikovetsky, P., 2017. Effects of fines migration on low-salinity waterflooding: analytical modelling. Transport Porous Media 116, 213–249.
Britannica, 2022. fabric-geology viewed 17 October 2022. https://www.britannica.com/science/fabric. viewed 17 October 2022.
Chen, X., Regenauer-Lieb, K., Lv, A., Hu, M., Roshan, H., 2020. The dynamic evolution of permeability in compacting carbonates: phase transition and critical points. Transport Porous Media 135, 687–711.
Chen, X., Li, Y., Liu, Z., Zhang, J., Trivedi, J., Li, X., 2023. Experimental and theoretical investigation of the migration and plugging of the particle in porous media based on elastic properties. Fuel 332 (Part 2), 126224.
Chequer, L., Bedrikovetsky, P., 2019. Suspension-colloidal flow accompanied by detachment of oversaturated and undersaturated fines in porous media. Chem. Eng. Sci. 198, 16–32.
Chequer, L., Vaz, A., Bedrikovetsky, P., 2018. Injectivity decline during low-salinity waterflooding due to fines migration. J. Petrol. Sci. Eng. 165, 1054–1072.
Civan, F, 2007. Temperature effect on power for particle detachment from pore wall described by an Arrhenius-Type Equation", in. Transport Porous Media 67, 329–334.
Coronado, M., Diaz-Viera, M.A., 2017. Modeling fines migration and permeability loss caused by low salinity in porous media. J. Petrol. Sci. Eng. 150, 355–365.
Davis, G., Reynolds, S., Kluth, C., 2011. Structural Geology of Rocks and Regions, third ed. Wiley, New York. ISBN: 978-0471152316.
Di Meglio, A., Giulio, E.D., Dragonetti, R., Massarotti, N., 2021. Analysis of heat capacity ratio on porous media in oscillating flow. Int. J. Heat Mass Tran. 179, 121724.
Ehlers, W., 2018. Effective stresses in multiphasic porous media: a thermodynamic investigation of a fully non-linear model with compressible and incompressible constitutents. Geomechanics for Energy and the Environment 15, 35–46.
Erias, A.F., Iglesias, E.M., 2022. Price and income elasticity of natural gas demand in Europe and the effects of lockdowns due to Covid-19. Energy Strategy Rev. 44, 100945.
Fegade, S.L., Tande, B.A., Cho, H., Seames, W.S., Sakodynskaya, I., Muggli, D.S., Kozliak, E.I., 2013. Aromatization of propylene over HZSM-5: a design of experiments (DOE) approach. Chem. Eng. Commun. 200, 1039–1056.
Fossen, H., 2010. Structural Geology, first ed. Cambridge University Press, New York. ISBN: 978-0521516648.
Geistlinger, H., Ataei-Dadavi, I., Vogel, H.-J., 2016. Impact of surface roughness on capillary trapping using 2D-micromodel visualization experiments. Transport Porous Media 112, 207–227.
Ghosh, S.K., 1993. Structural Geology: Fundamentals and Modern Developments, first ed. Pergamon, USA. ISBN: 978-0080418780.
Gokhale, N., 2019. Theory of Structural Geology, first ed. CBS, India. ISBN: 978-8123904535.
Goldenberg, L.C., Hutcheon, I., Wardlaw, N., Melloul, A.J., 1993. Rearrangement of fine particles in porous media causing reduction of permeability and formation of preferred pathways to flow: experimental findings and a conceptual model. Transport Porous Media 13, 221–237.
Gu, H., Wang, C., Gong, S., Mei, Y., Li, H., Ma, W., 2016. Investigation on contact angle measurement methods and wettability transition of porous surfaces. Surf. Coating. Technol. 292, 72–77.
Haasan, O.H., Sultan, G.I., Sabry, M.N., Hegazi, A.A., 2022. Investigation of heat transfer and pressure drop in a porous media with internal heat generation. Case Stud. Therm. Eng. 32, 101849.
Hamaker, H.C., 1937. The London–Van der Waals attraction between spherical particles. Physics 4, 1058.
Hills, E., 1963. Elements of Structural Geology, first ed. Chapman & Hall Ltd. ISBN: 978-0412207501.
Hobbs, B., Means, W., Williams, P., 1976. An Outline of Structural Geology, first ed. John Wiley and Sons. ISBN: 978-0471401575.
Huang, P., Shen, L., Maggi, F., Chen, Pan, Z., 2022. Influence of surface roughness on methane flow in shale kerogen nano-slits. J. Nat. Gas Sci. Eng. 103, 104650.
Hussain, F., Zeinijahromi, A., Bedrikovetsky, P., Badalyan, A., Carageorgos, T., Cinar, Y., 2013. An experimental study of improved oil recovery through fines-assisted waterflooding. J. Petrol. Sci. Eng. 109, 187–197.
Isah, A., Arif, M., Hassan, A., Mahmoud, M., Iglauer, S., 2022. Fluid-rock interactions and its implications on EOR: critical analysis, experimental techniques and knowledge gaps. Energy Rep. 8, 6355–6395.
Jameel, A., Naser, N., Emwas, A.-H., Dooley, S., Sarathy, S.M., 2016. Predicting fuel ignition quality using 1H NMR spectroscopy and multiple linear regression. Energy Fuels 30, 9819–9835.
Jiang, S., 2012. Clay minerals from the perspective of oil and gas exploration. In: Valaskova, M., Martynková, G. (Eds.), Clay Minerals in Nature - Their Characterization, Modification and Application, first ed. IntechOpen Limited, London, pp. 21–38.
Jiang, P.-X., Ren, Z.-P., 2001. Numerical investigation of forced convection heat transfer in porous media using a thermal-non equilibrium model. International Journal of Heat and Fluid Transfer 22, 102–110.
Kampel, G., 2007. Mathematical Modeling of Fines Migration and Clogging in Porous Media. Georgia Institute of Technology. PhD.
Kanimozhi, B., Bapu, B.R.R., Pranesh, V., 2017. Thermal energy storage system operating with phase change materials for solar water heating applications: DOE modelling. Applied Thermal Energy 123, 614–624.
Kanimozhi, B., Prakash, J., Pranesh, V., Thamizhmani, V., Vishnu, R.C., 2018. Fines surface detachment and pore-throat entrapment due to colloidal flow of lean and rich gas condensates. J. Nat. Gas Sci. Eng. 56, 42–50.
Kanimozhi, B., Thamizhmani, V., Pranesh, V., Senthil, S., Selvakumar, T.A., 2019a. Kaolinite fines colloidal flow in high temperature porous carbonate media during saline water injection. J. Petrol. Sci. Eng. 175, 775–784.
Kanimozhi, B., Prakash, J., Pranesh, R.V., Mahalingam, S., 2019b. Numerical and experimental investigation on the effect of retrograde vaporization on fines migration and drift in porous oil reservoir: roles of phase change heat transfer and saturation. J. Pet. Explor. Prod. Technol. 9, 2953–2963.
Kanimozhi, B., Mahalingam, S., Pranesh, V., Kesavakumar, R., Senthil, S., Ravikumar, S., Pradeep, S., Senthil, S., Murugan, R., 2020. Colloidal release in high temperature porous media with oversaturated fines during supercritical CO2 transport. J. Petrol. Sci. Eng. 192, 107345.
Kanimozhi, B., Rajkumar, P., Kumar, R.S., Mahalingam, S., Thamizhmani, V., Selvakumar, A., Ravikumar, S., Kesavakumar, R., Pranesh, V., 2021. Kaolinite fines colloidal-suspension transport in high temperature porous subsurface aqueous environment: implications to the geothermal sandstone and hot sedimentary aquifer reservoirs permeability. Geothermics 89, 101975.
Karakurt, I., Aydin, G., 2023. Development of regression models to forecast the CO2 emissions from fossil fuels in the BRICS and MINT countries. Energy 263, 125650.
Khalili, N., Uchaipichat, A., Javadi, A.A., 2010. Skeletal thermal expansion coefficient and thermos-hydro-mechanical constitutive relations for saturated homogeneous porous media. Mech. Mater. 42, 593–598.
Khanna, O.P., 2014. Material Science & Metallurgy, second ed. Dhanpat Rai Publications, New Delhi, pp. 320–455.
Khilar, K., Fogler, H., 1998. Migrations of Fines in Porous Media, first ed. Kluwer Academic Publishers, Dordrecht. ISBN: 978-90-481-5115-8.
Krull, F., Mathy, J., Breuninger, P., Antonyuk, S., 2021. Influence of surface roughness on the collision behavior of fines particles in ambient fluids. Powder Technol. 392, 58–68.
Kumar, G., Prabhu, K., 2007. Review of non-reactive and reactive wetting of liquids on surfaces. Adv. Colloid Interface Sci. 133 (2), 61–89.
Li, P., Zhang, J., Rezaee, R., Dang, W., Li, X., Fauziah, C.A., Nie, H., Tang, X., 2021. Effects of swelling-clay and surface roughness on the wettability of transitional shale. J. Petrol. Sci. Eng. 196, 108007.
Li, P., Yue, F., Wang, K., Zhang, H., Huang, H., Kong, X., 2022. Fully coupled thermos-hydro-mechanical modelling and simulation of a fluid-saturated porous medium under local non-equilibrium condition. Int. J. Heat Mass Tran. 195, 123195.
Lin, D., Hu, L., Bradford, S.A., Zhang, X., Lo, I., 2021. Pore-network modeling of colloid transport and retention considering surface deposition, hydrodynamic bridging, and straining. J. Hydrol. 603, 127020.
Liu, X., Tong, Z.-X., He, Y.-L., 2022. Enthalpy-based immersed boundary-lattice Boltzmann model for solid-liquid phase change in porous media under local thermal non-equilibrium condition. Int. J. Therm. Sci. 182, 107786.
Mahalingam, S., Pranesh, V., Kanimozhi, B., Thamizhmani, V., Selvakumar, T.A., 2019. Subcritical CO_2 effects on kaolinite fines transport in porous limestone media. J. Pet. Explor. Prod. Technol. 1–9.
Mateus, M.M., Bordado, J, M., dos Santos, R.G., 2021. Simplified multiple linear regression models for the estimation of heating values of refuse derived fuels. Fuel 294, 120541.
Mazumder, S., Tep, B., Pangtey, K., Mitra, D., 2019. Basement tectonics and shear zones in Cauvery Basin (India): implications in hydrocarbon exploration. In: Mukherjee, S. (Ed.), Tectonics and Structural Geology: Indian Context, first ed. Springer Nature, Switzerland, pp. 279–313.
Mehdizad, A., Sedaee, B., Peyman, P., 2022. Visual investigation of the effect of clay-induced fluid flow diversion on oil recovery, as a low-salinity water flooding mechanism. J. Petrol. Sci. Eng. 209, 109959.
Mukherjee, S., 2015a. Atlas of Structural Geology. Elsevier, Amsterdam. ISBN: 978-0-12-420152-1.
Mukherjee, S., 2015b. Petroleum Geosciences: Indian Contexts. Springer Geology. ISBN978-3-319-03119-4.
Murthy, H.P.S., Subrahmanyam, A.V., Bhaskar Rao, H.V., 1950. Studies on Indian refractory clays: Part IV-some clays from Madras State. Trans. Indian Ceram. Soc. 44, 82–88.
Naik, S., You, Z., Bedrikovetsky, P., 2015. Rate enhancement in unconventional gas reservoirs by wettability alteration. J. Nat. Gas Sci. Eng. 26, 1573–1584.

Neumann, A.W., David, Robert, Zuo, Yi, 2011. Applied Surface Thermodynamics, first ed. CRC Press, Boca Raton, FL.
Nguyen, T.K.P., Zeinijahromi, Z., Bedrikovetsky, P., 2013. Fines-migration-assisted improved gas recovery during gas field depletion. J. Petrol. Sci. Eng. 109, 26–37.
Nolte, S., Fink, R., Krooss, B.M., Littke, R., 2021. Simultaneous determination of the effective stress coefficients for permeability and volumetric strain on a tight sandstone. J. Nat. Gas Sci. Eng. 95, 104186.
Oliveira, M.A., Vaz, A.S.L., Siqueira, F.D., Yang, Y., You, Z., Bedrikovetsky, P., 2014. Slow migration of mobilized fines during flow in reservoir rocks: laboratory study. J. Petrol. Sci. Eng. 122, 534–541.
Pandya, K., Bulsari, S., Sinha, S., 2011. SPSS in Simple Steps. Dreamtech Press India, New Delhi. ISBN: 978-9350042519.
Passchier, C.W., Trouw, R.A.J., 2005. Microtectonics, first ed. Pergamon, India. ISBN: 978-3642441110.
Pranesh, V., Ravikumar, S., 2019. Heat conduction and liberation of porous rock formation associated with fines migration in oil reservoir during waterflooding. J. Petrol. Sci. Eng. 175, 508–518.
Pranesh, V., Balasubramanian, S., Kumar, R.S., Sakthivel, R., Rajkumar, P., Ravikumar, S., 2019. Kaolinite flakes and coal fines production in lignite core under ambient conditions: a case study of Neyveli Lignite Field at Cauvery Basin, Southern India. J. Nat. Gas Sci. Eng. 64, 72–80.
Prempeh, K.O.K., Chequer, L., Badalyan, A., Bedrikovetsky, P., 2020. Effects of the capillary-entrapped phase on fines migration in porous media. J. Nat. Gas Sci. Eng. 73, 103047.
Raha, S., Khilar, C.K., Kapur, P.C., Pradip, P., 2007. Regularities in pressure filtration of fine and colloidal suspension. Int. J. Miner. Process. 84, 348–360.
Rajkumar, P., Mahalingam, S., Jeyakumaran, N., Pranesh, R.V., 2020. Effect of Kaolinite Clay on the Sandstone Rock Permeability under Rich Gas Condensate Flow" in International Virtual Conference on Recent Trends & Innovations in Science, Engineering and Social Science. VHNSN College, Virudhunagar, Tamil Nadu, India, pp. 104–112.
Raman, K., Jaiman, R., Lee, T., Low, H., 2016. Lattice Boltzmann simulations of droplet impact onto surfaces with varying wettabilities. Int. J. Heat Mass Tran. 95, 336–354.
Rao, C.G., 1981. Carbonate/clay-mineral relationships and the origin of protodolomite in L-2 and L-3 carbonate reservoir rocks of the Bombay high field, India. Sediment. Geol. 29, 223–232.
Russell, T., Pham, D., Neishaboor, M.T., Badalyan, A., Behr, A., Genolet, L., Kowollik, P., Zeinijahromi, A., Bedrikovetsky, P., 2017. Effects of kaolinite in rocks on fines migration. J. Nat. Gas Sci. Eng. 45, 243–255.
Russell, T., Chequer, L., Badalyan, A., You, Z., Bedrikovetsky, P., 2018a. Effect of kaolinite content on formation damage due to fines migration: systematic laboratory and modelling study. The APPEA Journal 58, 743–747.
Russell, T., Wong, K., Zeinijahromi, A., Bedrikovetsky, P., 2018b. Effects of delayed particle detachment on injectivity decline due to fines migration. J. Hydrol. 564, 1099–1109.
Safiyari, M.H., Shavvalpour, S., Tarighi, S., 2022. From traditional to modern methods: comparing and introducing the most powerful model for forecasting the residential natural gas demand. Energy Rep. 8, 14699–14715.
Sazali, Y.A., Sazali, W.M.L., Ibrahim, J.M., Graham, G., Gödeke, S., 2020. Investigation of fines migration for a high-pressure, high-temperature carbonate gas reservoir offshore Malaysia. J. Pet. Explor. Prod. Technol. 10, 2387–2399.
Schembre, J., Kovscek, A., 2005. Mechanism of formation damage at elevated temperature. J. Energy Resour. Technol. 127 (3), 171.
Schembre, J., Tang, G., Kovscek, A., 2006. Wettability alteration and oil recovery by water imbibition at elevated temperatures. J. Petrol. Sci. Eng. 52 (1–4), 131–148.
Senthil, S., Ravikumar, S., Pranesh, V., 2019. Adiabatic behaviour of gas wells due to natural reservoir fines migration: analytical model and CFD study. J. Pet. Explor. Prod. Technol. 9, 2863–2876.
Sharma, V., Cali, Ü., Sardana, B., Kuzlu, M., Banga, D., Pipattanasomporn, M., 2021. Data-driven shorty-term natural gas demand forecasting with machine learning techniques. J. Petrol. Sci. Eng. 206, 108979.
Singh, P., 2013. Engineering and General Geology, 2d ed. S.K. Kataria & Sons, India. ISBN: 978-9350142678.
Sinha, M.K, Guha, S.K, 1990. "Mineralogical analysis of five plastic fire clays: Chemical analysis and x-ray diffraction studies". Trans. Indian Ceram. Soc. 49, 100–102.
Ting, H.Z., Bedrikovetsky, P., Tian, Z.F., Carageorges, T., 2021. Impact of shape on particle detachment in linear shear flows. Chem. Eng. Sci. 241, 116658.
Toshev, B.V., 2006. Gibb's thermodynamics of wetting. Int. J. Mech. Eng. Educ. 257–259.
Trauscht, J., Pazmino, E., Johnson, W.P., 2015. Prediction of nanoparticle and colloid attachment on unfavorable mineral surfaces using representative discrete heterogeneity. Langmuir 31, 9366–9378.
Twiss, R., Moores, E., 2007. Structural Geology, second ed. WH Freeman and Co. ISBN: 978-0716749516.
van der Stelt, T.P., Casati, E., Chan, N., Colonna, P., 2015. Technical equation of state models for heat transfer fluids made of biphenyl and diphenyl ether and their mixtures. Fluid Phase Equil. 393, 64–77.
Vaz, A., Bedrikovetsky, P., Fernandes, P.D., Badalyan, A., Carageorges, T., 2017. Determining model parameters for non-linear deep-bed filtration using laboratory pressure measurements. J. Petrol. Sci. Eng. 151, 421–433.
Wall, B.R.G., 2006. Influence of depositional setting and sedimentary fabric on mechanical layer evolution in carbonate aquifers. Sediment. Geol. 72, 203–224.
Wang, C., Bobba, A.D., Attinti, R., Shen, C., Lazouskaya, V., Wang, L.P., Jin, Y., 2012. Retention and transport of silica nanoparticles in saturated porous media: effect of concentration and particle size. Environ. Sci. Technol. 46, 7151–7158.
Wang, L., Dresen, G., Rybacki, E., Bonnelye, A., Bohnhoff, M., 2020. Pressure-dependent bulk compressibility of a porous granular material modelled by improved contact mechanics and micromechanical approaches: effects of surface roughness of grains. Acta Mater. 188, 259–272.
Weiguo, X., Shuyan, W., Huang, L., Qiang, W., Qinghong, Z., Huilin, L., 2016. Thermo-hydraulic performance of liquid phase heat transfer fluid (Therminol) in a ribbed tube. Exp. Therm. Fluid Sci. 72, 149–160.
Won, J., Kim, T., Kang, M., Choe, Y., Choi, H., 2021. Kaolinite and illite colloid transport in saturated porous media. Colloids Surf. A Physicochem. Eng. Asp. 626, 127052.
Wu, M., Chang, L., Zhang, L., He, X., Qu, 2016. Effects of roughness on the wettability of high temperature wetting system. Surf. Coating. Technol. 287, 145–152.
Xie, Q., Saeedi, A., Piane, C.D., Esteban, L., Brady, P.V., 2017. Fines migration during CO2 injection: experimental results interpreted using surface forces. Int. J. Greenh. Gas Control 65, 32–39.
Yang, H., Balhoff, M.T., 2017. Pore-network modeling of particle retention in porous media. Transport Phenomena and Fluid Mechanics 63, 3118–3131.
Yang, Y., Bedrikovetsky, P., 2017. Exact solutions for nonlinear high retention-concentration fines migration. Transport Porous Media 119, 351–372.
Yang, Y., Siqueira, F., Vaz, A., You, Z., Bedrikovetsky, P., 2016a. Slow migration of detached fine particles over rock surface in porous media. J. Nat. Gas Sci. Eng. 34, 1159–1173.
Yang, Y., You, Z., Siqueira, F.D., Vaz, A., Bedrikovetsky, P., 2016b. Modelling of slow fines migration and formation damage during rate alteration. In: SPE Asia Pacific Oil & Gas Conference and Exhibition. Society of Petroleum Engineers, Australia.
Yang, S., Russell, T., Badalyan, A., Schacht, U., Woolley, M., Bedrikovetsky, P., 2019. Characterization of fines migration system using laboratory pressure measurements. J. Nat. Gas Sci. Eng. 65, 108–124.
You, J., Lee, K.J., 2021. A pore-scale investigation of surface roughness on the evolution of natural fractures during acid dissolution using DBS method. Journal of Petroleum Gas Science and Engineering 204, 108728.
You, Z, Osipov, Y, Bedrikovetsky, P, Kuzmina, L, 2014. Asymptotic model for deep bed filtration", in. Chem. Eng. J. 258, 374–385.
You, Z., Yang, Y., Badalyan, A., Bedrikovetsky, P., Hand, M., 2016. Mathematical modelling of fines migration in geothermal reservoirs. Geothermics 59, 123–133.
Yu, B., Zhao, H., Tian, J., Liu, C., Song, Z., Liu, Y., Li, M., 2021. Modeling study of sandstone permeability under true triaxial stress based on backpropagation neural network, genetic programming, and multiple regression analysis. J. Nat. Gas Sci. Eng. 86, 103742.
Yuan, Yuehua, Randall Lee, T., 2013. Contact Angle and Wetting Properties. Surface Science Technologies, Netherlands: Springer. Print.
Yun, Y., Kim, T., Hwang, S., Oh, H., Kim, Y., Jeong, H., Kim, S., 2022. Prediction of liquid storage volumes and flow rates for gas wells using machine learning. J. Nat. Gas Sci. Eng. 108, 104802.
Zeinijahromi, A., Lemon, P., Bedrikovetsky, P., 2011. Effects of induced fines migration on water cut during waterflooding. J. Petrol. Sci. Eng. 78, 609–617.
Zeinijahromi, A., Vaz, A., Bedrikovetsky, P., 2012. Well impairment by fines migration in gas fields. J. Petrol. Sci. Eng. 88–89, 125–135.
Zeinijahromi, A., Farajzadeh, R., Bruining, J.H., Bedrikovetsky, P., 2016. Effect of fines migration on oil-water relative permeability during two-phase flow in porous media. Fuel 176, 222–236.
Zhang, H., Malgaresi, G., Bedrikovetsky, P., 2018. Exact solutions for suspension-colloidal transport with multiple capture mechanism. Int. J. Non Lin. Mech. 105, 27–42.
Zhang, L., Xu, C., Guo, X., Zhu, G., Cai, S., Wang, X., Jing, W., Sun, H., Yang, Y., Yao, J., 2021. The effect of surface roughness on immiscible displacement using pore scale simulation. Transport Porous Media 140, 713–725.
Zhou, Y., Yang, W., Yin, D., 2022. Experimental investigation on reservoir formation damage caused by clay minerals after injection in low permeability sandstone reservoirs. J. Pet. Explor. Prod. Technol. 12, 915–924.
Zoback, M.D., 2010. Reservoir Geomechanics. Cambridge University Press, Cambridge. ISBN: 978-0521146197.